THE FLUIDYNE HEAT ENGINE.

David Cottrell Mosby

NAVAL POSTGRADUATE SCHOOL
Monterey, California

THESIS

THE FLUIDYNE HEAT ENGINE

by

David Cottrell Mosby

September 1978

Thesis Advisors:
R. H. Nunn &
D. Salinas

REPORT DOCUMENTATION PAGE		READ INSTRUCTIONS BEFORE COMPLETING FORM
1. REPORT NUMBER	2. GOVT ACCESSION NO.	3. RECIPIENT'S CATALOG NUMBER
4. TITLE (and Subtitle) The Fluidyne Heat Engine		5. TYPE OF REPORT & PERIOD COVERED Master's Thesis September 1978
		6. PERFORMING ORG. REPORT NUMBER
7. AUTHOR(s) David Cottrell Mosby		8. CONTRACT OR GRANT NUMBER(s)
9. PERFORMING ORGANIZATION NAME AND ADDRESS Naval Postgraduate School Monterey, CA 93940		10. PROGRAM ELEMENT, PROJECT, TASK AREA & WORK UNIT NUMBERS
11. CONTROLLING OFFICE NAME AND ADDRESS Naval Postgraduate School Monterey, CA 93940		12. REPORT DATE September 1978
		13. NUMBER OF PAGES 97
14. MONITORING AGENCY NAME & ADDRESS(If different from Controlling Office) Naval Postgraduate School Monterey, CA 93940		15. SECURITY CLASS. (of this report) Unclassified
		15a. DECLASSIFICATION/DOWNGRADING SCHEDULE

16. DISTRIBUTION STATEMENT (of this Report)

Approved for public release; distribution unlimited.

17. DISTRIBUTION STATEMENT (of the abstract entered in Block 20, if different from Report)

18. SUPPLEMENTARY NOTES

19. KEY WORDS (Continue on reverse side if necessary and identify by block number)

energy conversion, heat engine

20. ABSTRACT (Continue on reverse side if necessary and identify by block number)

Laboratory tests were conducted on a small scale Fluidyne heat engine in the loaded and unloaded configuration to evaluate the effect of geometric changes on the system's operating characteristics. Liquid column displacements, gas temperature, and pressure were the primary variables measured for various heat inputs and gas volumes. Representative outputs were a pumping rate of 0.0976 gal/min through a head

DD FORM 1473 EDITION OF 1 NOV 68 IS OBSOLETE
1 JAN 73
S/N 0102-014-6601 |

of 0.825 ft, with a overall efficiency of .15%, and operating pressures as high as 5 psig. The results of the experimental program are presented together with a summary of the principles of operation.

The Fluidyne Heat Engine

by

David Cottrell Mosby
Lieutenant, United States Navy
B.S., Prairie View A. & M. University, 1970

Submitted in partial fulfillment of the
requirements for the degree of

MASTER OF SCIENCE IN MECHANICAL ENGINEERING

from the

NAVAL POSTGRADUATE SCHOOL
September 1978

ABSTRACT

Laboratory tests were conducted on a small scale Fluidyne heat engine in the loaded and unloaded configuration to evaluate the effect of geometric changes on the system's operating characteristics. Liquid column displacements, gas temperature, and pressure were the primary variables measured for various heat inputs and gas volumes. Representative outputs were a pumping rate of 0.0976 gal/min through a head of 0.825 ft, with an overall efficiency of .15%, and operating pressures as high as 5 psig. The results of the experimental program are presented together with a summary of the principles of operation.

TABLE OF CONTENTS

LIST OF FIGURES

LIST OF TABLES

NOMENCLATURE

English Letter Symbols

A_d — Cross-sectional area of displacer tube

A_{ij} — Tube cross-sectional area

C_d — Discharge coefficient

g — Acceleration of gravity, $g = 32.2$ ft/sec^2.

h_e — Equilibrium height of liquid

h_i — Liquid head

h_1 — Liquid level of water in cold column

h_2 — Liquid level of water in hot column

h_3 — Liquid level of water in output column

l_c — Equilibrium length of cold leg to output

l_d — Length of the displacer

l_h — Equilibrium length of hot leg to output

L_{ij} — Fluid inductance between points i and j $= \rho\, l_{ij}/A_{ij}$

l_{ij} — Tube length between i and j

P_c — Pressure of the container

P_{12} — Pressure of gas volume (1, 2)

P_a — Atmospheric gas pressure

P_∞ — Equilibrium gas volume pressure

Q_{ij} — Volumetric flow rate in direction i to j

R_{ij} — Fluid resistance (for laminar flow $R = 8\pi\mu l/A^2$)

R — Gas constant for Air, 53.34 ft-lbf/lbm-$^\circ$R

T_h — Gas temperature of the hot column

T_c — Gas temperature of the cold column

T_g — Temperature of the gas

T_1 — Cold gas temperature

T_2 — Hot gas temperature

V_g — Volume of the gas

V_e — Equilibrium volume of the gas

V_1 — Volume of cold gas

V_2 — Volume of hot gas

Greek Letter Symbols

ΔT — Critical temperature differential

ω — Oscillating frequency

μ — Liquid viscosity

ρ — Liquid density $lbf\text{-}sec^2/ft^4$

ACKNOWLEDGEMENT

I. INTRODUCTION

A. BACKGROUND INFORMATION

The Fluidyne heat engine was invented by C. West [1] in 1970 at the Harwell Laboratory of the United Kingdom Atomic Energy Research Establishment. The Fluidyne has the distinct advantage of producing work without the aid of any solid moving parts or rotating mechanisms, and is simple to fabricate.

The principle of operation is often approximated by a closed Stirling cycle, where two adjacent columns of liquid are stimulated into oscillation by the transfer of heat to and from a connecting volume of gas. Thermodynamically, the ideal cycle consists of two constant volume processes and two isothermal processes, as shown in Figure 1. The cycle is excited by the use of a heater and two liquid pistons, one of which displaces the gas back and forth between the hot and cold regions, and the other which provides the work output.

The pump can be self-starting on the application of heat, and will continue in operation as long as heat is supplied. It is felt that low grade heat is an adequate source of energy, including hot water, waste industrial heat, direct sunlight, or in temperate climates, concentrated sunlight.

There is great potential for further development of the design, particularly in small units for pumping irrigation

water in arid areas or for circulation pumps in hot water systems, including solar heated panels. A promising naval application is to provide standby power for pumps (emergency bilge pumps). Another potential application is to provide power for secondary controls in nuclear process plants by using the residual nuclear heat to operate a self-contained Fluidyne pump.

Insufficient understanding of the principles of Fluidyne operation has inhibited the improvement of the efficiency of engines utilizing this method. Present efficiencies are of the magnitude of 3 percent or less, which limits practical applications to those in which energy is available at no cost, such as solar energy [2], and waste heat. Several analytical models have been developed by various individuals, however all of these models are limited by their respective assumptions.

The overall objective of this investigation has been to provide experimental evidence, in various forms, to assist in developing and validating more accurate analytical descriptions of the Fluidyne process. This thesis presents an overview of the process, as it is presently understood, followed by a detailed description of the experimental efforts and the results obtained.

B. THE BASIC FLUIDYNE

The sequence of cycle events can be described by referring to the basic Fluidyne machine in Figure 2, where the pistons

are in the form of liquid columns. A mass of gas is confined above three of these columns, with the fourth exposed to the atmosphere. As the liquid in the lefthand U-tube oscillates, gas is displaced between the hot and the cold cavities formed in the spaces above the liquid and flowing through the regenerator. As the right hand liquid column oscillates the total volume of the gas is altered.

If the hot cavity volume change leads the cold cavity by other than 180 degrees, the pressure change has a component in phase with the velocity of the output column and this component can be used to overcome viscous friction in the output tube and do external work. The problem is to maintain the amplitude and phase of the liquid in the displacer tube in the presence of viscous losses. Three methods of returning some of the available output power to the displacer have been tested and the engines are classified according to the method of achieving this feedback [1].

In general the displacer and output are intended to be two mechanically resonant circuits and must be correctly tuned for satisfactory operation. The brief descriptions that follow are derived from the material presented in references 1, 2, and 3.

C. FEEDBACK RESPONSE

   1. Rocking Beam Feedback

       This is conceptually the most easily understood method. However, because it involves a moving part, the full advantages

15

of the liquid piston scheme are not fully realized. This arrangement is shown in Figure 3. The entire engine is pivoted such that it can swing in the plane of the paper about point C. As the liquid in the output column commences oscillating, the center of gravity shifts and the entire assembly moves against a restoring force offered by the spring. This rocking action maintains the oscillation of the displacer liquid. An experimental engine operating on this type feedback has been built and successfully tested [1] using water in the displacer and mercury in the output.

    2. Pressure Feedback

        In this system the two cold cavity volumes (displacer and output) are combined. Figure 4 displays this arrangement. If care is taken in selection of tube lengths and diameters the phasing between the motions of the hot and cold columns can be controlled. This feedback phenomenon has also been proved experimentally utilizing water throughout [1].

    3. Jet-Stream Feedback

        Two cold cavities are again combined, as in Figure 5. The liquid flowing into the displacer U-tube from the output tube feeds energy into the displacer liquid in a way that is similar to the action of a jet pump.

        This arrangement as well as the pressure feedback both share the advantage of requiring no solid moving parts.

        Figure 6 is yet another variation of the jet-stream feed-back system. As shown, the majority of the output tube is

contained within the envelope of the reservoir which presents the possibility of a very compact assembly. In this configuration, the displacer tube has been replaced with a fluid reservoir. Dynamic head feedback from the output to the hot column plays a significant role in the pump's operation, in that the inertia of the moving fluid in the output leg preferentially acts to continually change the head in the hot column.

Figure 7 shows the overall experimental setup used during this thesis project, in which it can be seen that the Fluidyne configuration closely resembles that of Figure 6, and thus operates on the jet-stream feedback principle. Selection of this geometry for further study was based upon the recommendation of the inventor [1].

D. EXPERIMENTAL OBJECTIVES

There were five primary experimental goals set forth at the beginning of this project.
They were as follows:

1) To fabricate a Fluidyne system.

2) To prove the Fluidyne system operational.

3) To instrument the system for the recording of pertinent data.

4) To establish operating parameters and observe characteristics peculiar to the system's operation in it's unloaded configuration.

5) To observe and record significant data regarding
   the system's behavior in the loaded condition.

In addition, it is hoped that this work will provide a
basis for additional experimentation and improvements, thus
encouraging the construction of Fluidyne replicas in educa-
tional and research laboratories.

Before proceeding with a discussion of the experimental
program, a brief review of the operation of the Fluidyne,
as it is presently understood, is presented.

II. THEORY OF OPERATION

A. PHYSICAL DESCRIPTION OF START-UP PHENOMENON

Figure 8 is a simplified representation of the model
actually tested, and is therefore used to describe the prin-
ciple of operation. Shown is a reservoir of liquid with a
connecting U-tube of gas branching between the columns of
displacer liquid. An additional U-tube filled with the same
liquid is arranged such that one end loosely fits into the
hot column and the other end is open to the atmosphere.
Essentially this configuration represents the Fluidyne in
it's unloaded condition with the output column exposed to a
constant ambient pressure.

It is hypothesized that the gas volume remains in two
separate imaginary halves during operation. The right half,
labeled 2, which is hydrodynamically coupled to the output
tube is the hot region, and the left, labeled 1 is the cold
region. In the series of experiments conducted, an insulated
heating coil was used to obtain desired temperatures in the
hot region and the temperature in the cold region was main-
tained approximately constant through convection and conduc-
tion to the ambient surroundings.

The start-up and subsequent steady-state oscillating
condition may be described in five phases, as pictorially
described in Figure 9.[1]

---

[1]The author wishes to acknowledge the contributions of Mr.
T. Drzewiecki of the Harry Diamond Laboratories, whose insights
have led to the start-up descriptions provided here.

In Phase I, the initial phase, no heat is applied. The liquid levels h_1, h_2, and h_3 are all determined by the static pressure in the gas volume. Liquid levels h_1 and h_2 are equal, and if the gas pressure P_{12} is ambient, then $h_1 = h_2 = h_3$. Figures 9a and 10 further exemplify this condition.

Phase II begins with a new equilibrium condition. Liquid levels h_1 and h_2 are equal, but may not necessarily be equal to h_3 as seen in Figures 9b and 11. This is due to pressurization of the gas volume which may occur, for instance, during assembly of the apparatus. Heat is applied to the right half of the gas volume (2) causing an increase in the volume V_g and the pressure P_{12}. The gas temperature T_g in (2) also increases with that in (1) remaining close to ambient conditions. Liquid levels h_1 and h_2 decrease thus h_3 increases. The accelerations in the three liquid columns are time dependent.

During Phase III, thermal equilibrium in the gas is approached. The inertia of the fluids in levels h_1 and h_2 keeps them moving down and that in column h_3 keeps it moving upward. Gravity overcomes the acceleration in h_3, the output leg, and thus the motion in this leg stops momentarily (Figure 9c).

Phase IV picks up at this point with h_2 and h_3 tending to seek the same level under the force of gravity. Hence h_2 now increases and h_3 starts to decrease. There is a reduction in the average gas temperature since less gas is exposed to the heat source (Figure 9d). The pressure P_{12} also decreases.

20

All of these changes are augmented by the descent of the output level due to gravity which produces a dynamic head at the base of (2) further increasing h_2. An overshoot of the two liquid levels occurs, h_2 greater than h_1, with h_3 less than h_2, which again gives rise to a gravity potential between liquid levels.

Finally, in Phase V the liquid levels again seek equilibrium with level h_2 decreasing. This exposes more gas to the heat source causing the gas to once again expand and the cycle begins all over again with the output liquid level traveling in the upward direction. In a properly tuned system, steady state oscillation is achieved from this point on. Figure 12 represents a still photo of the Fluidyne operating in a steady state condition.

B. MATHEMATICAL ANALYSIS

A mathematical analysis of the Fluidyne liquid piston engine has been given by both West [1] and Elrod [2]. Geisow [3] likewise proposed a set of governing equations for a lossless Fluidyne system in an attempt to compute the necessary conditions for the onset of oscillations. All of these early analyses have been of the small-disturbance type, and they offer only limited information concerning the steady state operation where the assumption of small disturbances is not valid. The assumptions applicable to the early inviscid analyses are as follows:

21

1) Air and water are the work media.

2) No losses and the system performs a true Stirling cycle.

3) The working gas is ideal.

4) The equilibrium pressure is equal to atmospheric pressure.

5) Friction in the liquid is neglected.

6) The pressures in the hot and cold cylinders are equal.

7) The temperatures in the hot and cold legs are uniform at any given instant of time.

8) Constant cross sectional area for the displacer.

Geisow [3] utilized the Euler equations of motion in one dimension, linearized them and performed a first order pertubation stability analysis. The results of this analysis led to expressions for the critical temperature differential ΔT and the oscillating frequency ω as functions of geometry and the thermodynamic properties.

Equations (1) and (2) analytically describe this temperature and frequency condition.

$$\frac{\Delta T}{T_1 + T_2} = \frac{\rho g V_e}{2A_d P_a} \left(\frac{l_c - l_h}{l_d}\right) \tag{1}$$

$$\omega = \left[\frac{2g}{2l_h + l_d \left(\frac{A_c}{A_d}\right)}\right]^{\frac{1}{2}} \tag{2}$$

This analysis was performed for the geometry shown in Figure 13 and further indicates a strong dependency of the system response on the geometry of the displacer tube.

Relationship (2), which gives the ideal threshold frequency, implies free oscillations in the displacer U-tube circuit, with no liquid movement in the output tube. Thus, logically enough, a minimum threshold temperature difference is required for self-excited oscillations even with zero work output. The small-disturbance analysis indicates, for instance, that the Fluidyne pump should be able to operate with a heater temperature of about $185^{\circ}F$ and a cooler temperature of $100^{\circ}F$, with the anticipated working frequency close to 1 Hz. These operating conditions are representative of those obtained in the experiments described herein.

The neglect of friction in the liquid leads to under-estimates of the threshold temperature differences. However, at high frequencies and small amplitudes of oscillation, frictional effects are not likely to be appreciably large. For instance at a typical working frequency of 1 Hz, the effects of wall friction in water occur inside a boundary layer less than .08 inches thick [2]. In addition, for oscillatory disturbances of small amplitude, the formation of separation regions is inhibited. Finally, the length-diameter ratios of the various segments of the liquid conduit are large enough to justify the approximation of one-dimensional flow.

The gas side of the Fluidyne system is more difficult to analyze. It is true that the low density and viscosity of gases permit the simple assumption of equal pressures in the

23

hot and cold regions. But at heater operating temperatures, the saturation pressure of water becomes appreciable. Although the presence of non-condensable air prevents the heater and cooler interconnection from becoming a thermosyphon, there certainly will be inhomogeneity within the gas mixture, and consequently there will be complicated two-phase mechanisms operative on all active heat transfer surfaces. In view of these complications, the assumption made by West [1] seems warranted for the present, that any gas in the cooler is always at some fixed lower temperature of T_1 and that of the heater always is at temperature T_2.

The original Fluidyne did in fact possess a configuration as previously described (Figure 13), however current emphasis seems to be on configurations that utilize jet-stream feedback.

In this section, the recent analysis due to T. Drzewiecki [4] is reviewed. This analysis applies whether the geometry is that of Figures 8 or 14. The pressure drop $P_{ij} = P_i - P_j$ for any tube can be written for time-varying slug flow as

$$P_{ij} = L_{ij} \frac{dQ_{ij}}{dt} + R_{ij} Q_{ij} + h_i \rho g \qquad (3)$$

It follows that for the cold column between points (1) and (3), for instance (refer to Figure 8), the pressure drop becomes

$$P_3 - P_1 = L_{13} \frac{dQ_{31}}{dt} + R_{31} Q_{31} + h_1 \rho g \qquad (4)$$

Similiarly, the hot column and output column pressure drops can be written with an additional pressure feedback term included due to the dynamic head effect of the output column. This effect gives rise to a difference in pressure between the bases of the hot and cold legs, which can be expressed as

$$P_4 - P_3 = \rho \; Q_{31}^2 \; / \; (2 \; (A_{42} - A_{45})^2 \; c_d^2) \qquad (5)$$

This in effect treats the region where the output column extends into the base of the hot column as an orifice resistance. Otherwise if the output tube did not impede flow from the reservoir, P_3 would be equal to P_4.

The liquid heights and the volume flow rates are simply related by

$$A_{ij} \frac{dh_i}{dt} = Q_{ij} \qquad (6)$$

and from the conservation of mass of an incompressible fluid, the net flow into the reservoir must be zero or

$$Q_{31} + Q_{42} + Q_{45} = 0 \qquad (7)$$

For the analysis of the unloaded system, P_5 is considered to be ambient and constant. If the assumption is made that the pressure is uniform at any instant of time in the gas volume (the viscous resistance in the gas thus being neglected) then

$$P_1 = P_2 \qquad (8)$$

The gas mass must likewise be conserved so that

$$m_1 + m_2 = \text{constant} \qquad (9)$$

Since it is assumed that the gas is ideal, the equation of state may be written for each side of the gas volume.

$$p_1 V_1 = m_1 R T_1 \qquad (10)$$

$$p_1 V_2 = m_2 R T_2 \qquad (11)$$

The gas volumes are directly related geometrically to the position of the gas liquid interface such that

$$V_1 = \tfrac{1}{2} V_e - (h_1 - h_e) A_{13} \qquad (12)$$

$$V_2 = \tfrac{1}{2} V_e - (h_2 - h_e) A_{24} \qquad (13)$$

The heat transfer processes within the gas volume are complex to the extent that only the most simple expressions have been used for T_1 and T_2. Thus, for example,

$$T_1 = \text{Constant} \qquad (14)$$

$$T_2 = \text{Constant} \qquad (15)$$

where T_1 and T_2 are average temperatures in each volume of gas.

Upon examination of these governing equations, one notes that the pressure-drop equations are nonlinear since both the inductance and resistance terms are functions of the lengths of the liquid columns. Linearization could be achieved by

stipulating that the total excursions of the liquid interfaces
are considerably smaller than the equilibrium lengths, however
this can be an unrealistic departure from fact.

Equations (3) - (15) have been cast into a computer program
and solved simultaneously without resorting to perturbation
or threshold analyses. At the present time the solution of
the equations by computer, an effort outside the scope of this
thesis, has not yielded results that are completely satisfactory.

III.   EXPERIMENTAL APPARATUS

The equipment used in performing the experiments conducted within this thesis is illustrated in Figure 7. Shown, left to right, is the temperature controller, Fluidyne pump, and the oscillograph. Located above the oscillograph is a strip-chart recorder and digital pyrometer. Brief descriptions of this equipment are provided below.

A.   CONTROLLER

The controller is a Model 49 proportioning controller. This model automatically proportions the relay on and off time in accordance with the demand of the process. The pro-portioning action occurs within a band around the set point called the proportioning band. The Model 49 bandwidth is 2 percent of scale range. Within this band, various on-time to off-time ratios occur. At the very edge of the band, below set point, power to the heaters is on 100% of the time. As the controlled temperature enters the proportioning band, the on-time decreases steadily until the upper edge of the band is reached, where the on-time would be 0%. The adjusted on to off time ratio allows the controller to proportion the heat on and off without a change in the actual controlled temperature. In this way uniform process temperature control is approximately achieved.

While most controls of this type have a fixed or manually adjusted proportioning time cycle, this model features automatic rate action which varies the cycle time in accordance with the demands of the process. Detailed specifications are listed in Appendix E.

B. FLUIDYNE ASSEMBLY

The Fluidyne pump as illustrated in Figure 15, is comprised of a coiled output line, three displacement columns, a connecting gas tube, heating coil, and an output valve. The dimensions presented in this figure represent the actual size of the model used in the conduct of the experiments.

All glass parts were fabricated of Pyrex glass. Tygon and Poly-Flo tubing was used for the output and connecting gas tube respectively. The coiled output line consisted of eight coils with an ID of 0.4 inches, and an approximate length of 70 inches. The reservoir which houses these coils was approximately 153 cubic inches in volume. The hot and cold displacement columns were 0.620 inches ID and 7 inches in length for this particular setup. The connecting gas tube length varied during different runs, however a constant ID of 0.185 inches was maintained.

The heating coil material was Aluminum. However 1-inch insulation was used on all faces to reduce heat losses. Holes were provided for installation of the coil as well as the heater elements.

The pump assembly was purchased as a complete unit with non-return valves already installed.

C. INSTRUMENTATION

One of the most critical components of an experimental apparatus is the instrumentation. In the case of the Fluidyne, accuracy and sensitivity of measuring instruments is required because of the temperature difference associated with a small change in displacement, and the complexity involved in analyzing the gas/water interaction. The instrumentation used in this experimental study is reviewed in the following paragraphs.

1. Displacement

A four channel water-level indicating system was used to monitor the displacement levels of the water inside each column. This device consisted of a single high-level driver-oscillator and four identical but independent sensing circuits. Each channel provided for zero offset, and variable gain via two panel-mounted pots with ten-turn indicating dials.

The dynamic response of the electronics was essentially flat to 1 KHz. The sensing method was variable capacitance.[2] Thirty-gauge enameled magnet wire was used as the sensor with outputs obtainable from 0.010 to 40 inches. This wire, which

---

[2]The displacement measuring system, as well as a large portion of the instrumentation system, was designed and built by Mr. T. Christian of the Mechanical Engineering Department.

30

functioned as one plate of a capacitor, was sealed with "Glyptal" on the cut end which was immersed in the water, to prevent a d.c. path from being completed through the water. Ordinary tap water, sea water or any other solution which contains dissolved minerals will function as the other plate of the capacitor. (Distilled water will not work, as it is not conductive.)

The inner surface of the container should be conductive, and acts as the ground return. However in the case of glass containers or long glass tubes as used in these experiments, it was necessary to install an additional bare Copper wire at a uniform distance from the actual probe wire to serve as the ground return.

It is very important that the return wire be kept clean of corrosion or residue of any foreign material which will inhibit conductance. The probe wire discussed exhibits roughly 10 picofarads change in capacitance for a one inch immersion. In this configuration as long as the total probe capacitance remains less than 1000:1 ratio to the bridge capacitors (0.056 mfd), dependable linear outputs may be realized.

During the operation of this system a 10 KHz sine wave is used to excite an RC bridge, with a sensor probe placed in parallel with one of the capacitors in the lower half of the bridge. As the water level increases, more of the

surface area of the water covers the probe, increasing the effective capacity of that leg of the bridge.

Calibration was accomplished by immersing the probe in a measured level of liquid and observing the resultant voltage change. Zero-position and gain adjustments were also available. Therefore the probe was cycled between the zero point selected and the positive and negative full scale points which were anticipated.

The bridge outputs were recorded on the multichannel oscillographic recording system shown in Figure 7.

2. Temperature

The temperature was monitored using a Digital Pyrometer Model 267 and strip-chart recorder. The Digital Pyrometer receives thermocouple inputs and displays them in degrees Fahrenheit. The thermocouple wire used was Type "T", Copper-Constantan, manufactured by Omega with the following limits.

Temperature Range $^{\circ}$F	Limits of Error
-300 to -75	$\pm$ 1%
-150 to -75	$\pm$ 1%
-75 to +200	$\pm$ 3/4 F
200 to 700	$\pm$ 3/8 %

The above limits of error are based on a reference junction temperature of 32°F. Fabrication was achieved using an inert gas welder. The thermocouples were mounted on the bottom side of the sealing stoppers in both the hot

and cold columns. Only the hot and cold gas temperatures were monitored during operation.

Outputs were recorded on the strip-chart recorder that can be seen in Figure 7.

3. Pressure

Pressure instrumentation was provided to measure the pressures inside the gas region. This was made possible through a Celesco Model KP-15 Pressure Transducer used in conjunction with a CD-10 Carrier Demodulator. This unit was installed midway within the connecting gas tube, and all measurements were recorded in that position. Pressure measurements were recorded only in the unloaded configuration. Additional specifications for this instrument are listed in Appendix E. The CD-10 Carrier Demodulator was designed to be used with the pressure transducer, to produce a d.c. signal output proportional to both steady state and dynamic parameters sensed by the transducer. Specifications for this unit are also listed in Appendix E.

The pressure transducer and associated demodulator were both calibrated in the laboratory against a water manometer with an accuracy to ± 1/10 inch.

IV. DATA COLLECTION PROCEDURES

Various data recording techniques were utilized prior
to final instrumentation. Initially, all displacement
heights were recorded through visual observation. The
maximum and minimum heights in all columns were observed
with the aid of a straight-edge for measurements, and these
values recorded for amplitudes. The temperature, on the
other hand, was simply recorded on a Digital NUMATRON for
any given instance of time. A Variac was utilized to supply
the power to a non-insulated coil assembly which ultimately
supplied the source of heat for the system. Time increments
of one minute were used for recording the data. No accurate
means of determining the frequency or phase angle was available
during this preliminary work. Qualitatively, many interesting
operating characteristics were observed and recorded during
this experimentation period, which led to future improvements.

Since it was felt that the gas temperature was a primary
variable it was decided to try and observe it's variation
with time. To assist in this setup, thermocouples were
mounted on the bottom side of the sealing stoppers and a
strip-chart recorder was connected to graphically display
these temperatures. See Figures 16-18 for sample recordings.

After the temperature was studied extensively, and it
was felt that the range and behavior of temperatures necessary
for operation were fairly predictable, an attempt was made

to accurately measure the displacements of the liquid columns.
An oscillograph as seen in Figure 7 was utilized for this
function. Thirty-gauge enameled magnet wires immersed in
each column sensed the displacement levels as a function of
time and provided a display of this behavior on the oscillo-
graph chart output. Following calibration, a given number
of lines on the chart output corresponded to so many inches
of water height in the columns. Thus the output, cold and hot
column displacement heights were then obtainable to an accept-
able degree of accuracy.

To maintain a reasonably constant temperature over a
period of time, the Variac was replaced with a controller
whose range varied from 0° to $300^{\circ}F$. Furthermore the heating
coil was insulated to minimize any heat losses, and the
experimental facility was relocated to a laboratory area
where the environmental conditions were substantially constant.

Frequency and phase-angle determinations were made possible
through data such as those illustrated in Figures 19-22.
Since the chart speed was readily obtainable from the oscillo-
graph, reduction of these data was a simple but time-consuming
task. Reduced data are listed in Tables I and II.

Pressure determinations were made possible through the
use of a pressure transducer, which was installed in the
midway region of the gas volume. Again the output was dis-
played on the oscillograph. See Figure 23.

Data concerning the pumping performance of the system
was obtained using a stop watch. Flow rates were determined
by timing a designated quantity of pumped water through a
fixed head, and recording temperature variances throughout
this period. Data results are shown in Tables III, IV, and V.

V. DISCUSSION OF EXPERIMENTAL RESULTS

A major portion of the experimental work was devoted to obtaining an operating machine built on the Fluidyne principle. Following the accomplishment of this goal, it was necessary to select parameters for experimental study such that useful results could be obtained within the allotted period of time. Accordingly, attention was focussed upon the gas volume and several series of experiments were conducted to investigate the effect and/or behavior of the temperature, pressure, and volume on this region. During these tests, the configuration of the device was otherwise left unchanged.

A. TESTS AT VARIOUS INITIAL GAS VOLUMES, TEMPERATURE HELD CONSTANT

The experimental results obtained are graphically displayed in Figures 17 through 28 and summarized in Tables I through XI. When several gas volumes were tested at a given temperature it was found that the output displacement decreased with increasing volume to a point where either it died out or additional heat was required to permit sustained operation. See Figure 24 for evidence of this behavior. This result is also supported by Table VI, which shows that as the volume increases the temperature required for the onset of oscillations also increases. Figure 24 also shows that at a temperature of

approximately 160°F, the output displacements[3] remain reasonably constant up to a critical volume of around 0.740 cubic inches. Beyond this point additional heat is required to produce an identical amount of displacement.

No volumes were tested below 0.5233 cubic inches due to the length restriction of the connecting gas tube. Temperatures were limited to 160°F for the variable volume runs, due to oscillations restrictions inside the hot and cold columns. Since the thermocouples were mounted on the underside of the sealing stopper in both columns, any splashes against them would have recorded false gas readings.

All gas volumes were achieved by varying the length of the connecting gas tube and maintaining the equilibrium levels inside the hot and cold columns constant. A liquid level height of 5.18 inches measured from the top of the closed container was the operating water level inside the hot and cold columns for all runs. This height is illustrated in Figure 15. This particular water level was chosen also because it afforded the greatest displacements in all columns without allowing the water inside the hot and cold column to contact the thermocouples.

---

[3]All liquid level data presented in this report are given as peak-to-peak values.

B.   TESTS AT VARIOUS GAS TEMPERATURES

Figures 25-27 are plots of the results obtained with various volumes held constant while varying the temperatures. All of the data show that output displacement increases linearly with temperature within experimental uncertainty. In other words, to obtain a greater work output more energy is required from the driving source. Even though these curves are approximately linear, reduced data scatter would result if strict temperature control were possible. The controller maintained a reasonably stable temperature, however strict adherence was next to impossible even with the coil insulated. Also worth noting is that the maximum output displacement was achieved utilizing the largest volume and temperature. Apparently, the dominant effect of the gas volume is that of limiting the maximum allowable gas temperature. In addition, the effects of vapor production at higher temperatures are less significant with the larger gas volumes. For instance, with the smallest volume of 0.523 cubic inches it was only possible to produce displacements of 11.9 inches at 184^OF whereas the largest volume (0.8458 cubic inches) allowed a temperature of 194^OF and the corresponding output displacement was 14.0 inches.

C.   FREQUENCIES AND PHASE ANGLES

In Figures 19-22 and Tables I, II, and VIII, one sees the variation of displacement and frequency of oscillation for

different parameter values. Increasing the hot gas temperature leads to a slight decrease in frequency. This result is attributed to the higher mean pressure in the gas which results in a larger volume and hence a slightly increased gas capacitance.

The odd-shaped waveforms shown for the output column, Figures 19-23, is not the true column-height versus time, but a distorted signal resulting from effects of the length and position of the sensing wires inside the output column at various times. For this reason the actual output displacement values used herein for data purposes were not taken from the readouts such as those shown in Figures 19-23, but were re-corded through visual measurement with results shown in Tables IX - XI.

Phase angles between the cold and hot column as well as the cold and output column were estimated from the waveforms. These values are summarized in Table II, and show a strong dependency on temperature and gas volume. The optimum con-dition would appear to be a phase angle of 180° between the cold and hot column. The data approach this value as the gas volume decreases.

D. PRESSURE IN THE GAS VOLUME

Figure 23 presents information concerning the pressure measurements inside the gas volume. The peak-to-peak variation of this pressure, which is influenced by the rise and fall

of the output column, is 2.53 psig for the particular volume
and temperature case cited. Furthermore, it was experimentally
determined that the gas pressure increased with an increase
in mean temperature. During the limited number of experiments
in which gas pressures were measured, pressures as great as 5
psig were observed.

E. TIME VARIATION OF GAS TEMPERATURE

Temperature vs time profiles are displayed in Figures 16-18.
From these plots it is seen that after the onset of oscilla-
tions, the temperature continues to rise to a point where a
short cooling period commences. During this cooling phase,
the output displacement decreases to a condition where less
heat is transferred from the gas and the temperature commences
to increase again until steady state operation is eventually
obtained. Also noted is the fact that increasing the volume
requires an increase in time prior to the commencement of
oscillations. All temperature plots were obtained by setting
the controller at a value much higher than the temperature
anticipated for onset of oscillation. For the particular cases
cited herein, the controller settings were $200^{O}F$. For instance,
Figure 18 shows that steady state oscillations were obtained
at a temperature of approximately $181^{O}F$, with the onset of
oscillations occurring after 2.88 minutes at a temperature of
$171^{O}F$.

Table VI in conjunction with Figure 28 gives data for predicting the onset of oscillations. All onset temperatures were obtained as a result of the system being heated from a cold-start ambient temperature of approximately 72^OF. It was discovered that these onset temperatures were considerably lower if the heating coil was initially warm. This is thought to be due, at least in part, to the energy expended in heating the insulated coil as well as the walls of the tubes. Onset temperature differences due to this effect were as much as 8^OF.

F. OPERATION IN THE LOADED CONFIGURATION

Finally, Tables III-V furnish some preliminary information concerning the pumping characteristics of the system. A fixed gas volume of 0.6308 cubic inches was used in all runs since the temperature required to produce sustained oscillations in the loaded condition for this particular volume ranged from 160° to 190^OF. Also it afforded a longer operating period prior to complete saturation of the gas in the connecting tube. The highest flow rate obtainable was 0.0976 gal/min which occurred at a pumping head of 9.9 inches. The highest measured overall efficiency was 0.149% (see Appendix C). Although this value is extremely low, it compares with that obtained previously [2] and it is felt that with continued research as suggested in Section VII, the efficiency can be improved upon.

VI.   CONCLUSIONS

The realization of an engine using liquid pistons to
achieve the required gas displacements and mechanically
tuned liquid columns to ensure correct phasing has been
shown to be theoretically and practically feasible. Indeed
such a device which offers potentially low cost and high
reliability may be of value to the underdeveloped areas of
the world, as well as the U.S. Navy.   Other applications
could be found in situations where heat is more readily
available than electricity.

A theoretical basis for design has been sketched out,
although it is clear that a full understanding of the inter-
action between various machine parameters has yet to be
achieved.

The trends and interdependency of geometric parameters
were discussed in detail in Section VI, and the resulting
conclusions are summarized here.

A.   Simultaneously increasing the temperature and gas
volume increases the output displacement.

B.   Increasing the gas volume at a constant temperature
decreases the output displacement.

C.   There is a slight cooling period after the onset of
oscillations. This is followed by a further temperature
increase prior to steady state operation.

D.   The frequency of output oscillation decreases with an
increase in gas temperature.

E.   In the loaded and unloaded configuration, the operating
frequency remained reasonably close to 1 Hz for the Fluidyne
configuration of this experiment.

F.   Decreasing the volume at a constant temperature
decreases the phase angle between the hot and cold columns.

G.   Higher temperatures are required for sustained opera-
tion in the loaded configuration than in the unloaded condition.

H.   Pressures in the gas volume were significantly higher
than those expected from hydrostatic heads alone. This result
indicates that significant dynamic pressure feedback was
present in the experimental model.

VII.   RECOMMENDATIONS

In addition to providing insight into the nature of the effects of geometric parameters on the Fluidyne's performance, this research also has raised questions to be answered by further research. Presented below are recommendations for improving upon the experiment and furthering a productive investigation into the performance of the Fluidyne.

A.   Variation of the geometric parameters was limited by the restrictions inherent in the original design. Although the number of geometrical variations are virtually unlimited, those of significant interest for further research include varying the area of the output, cold, and hot columns as well as the connecting gas volume. This will require major alterations to the existing system.

B.   In order to avoid the sensing of distorted waveforms, particularly in the output column, some means of maintaining the sensing wires inside all tubes perfectly straight and taut, must be devised.

C.   Since the oscillograph is non-supportable with replacement parts, it is recommended that a new recorder be obtained with at least eight channel capability.

D.   Some means of minimizing the accumulation of water vapor in the connecting gas tube must be developed since the system terminates operation when this area becomes saturated. This is particularly annoying when working with smaller volumes in the loaded configuration.

E.   The effects of heat transfer limitations, including thermal losses through the walls of the machine and through the movement of heated portions of the liquid, needs further study.
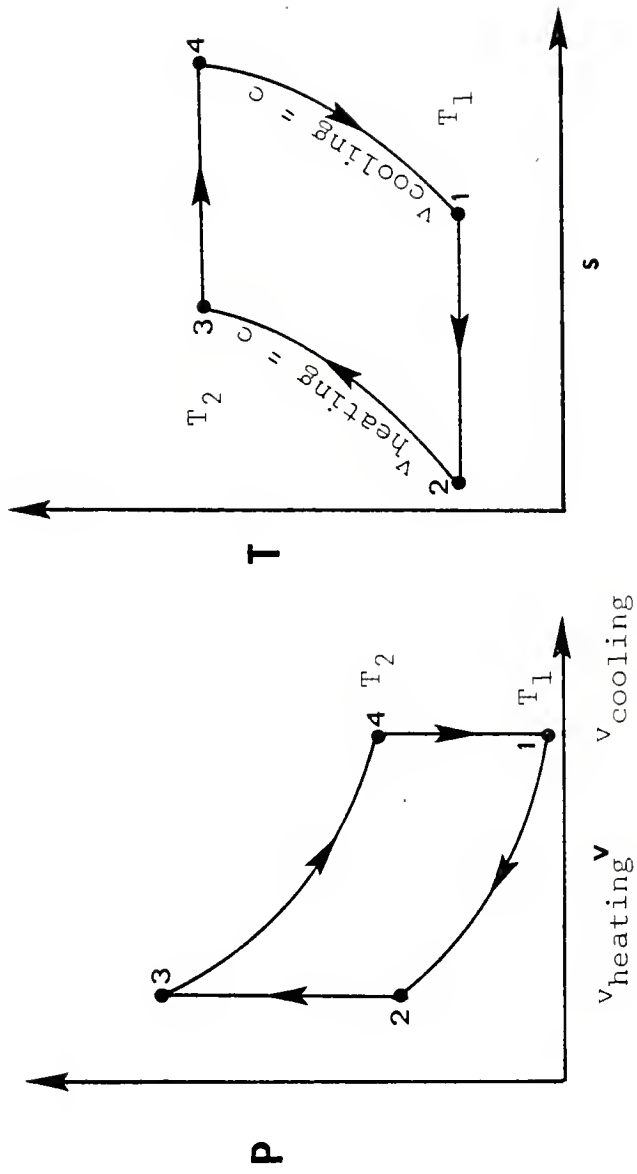
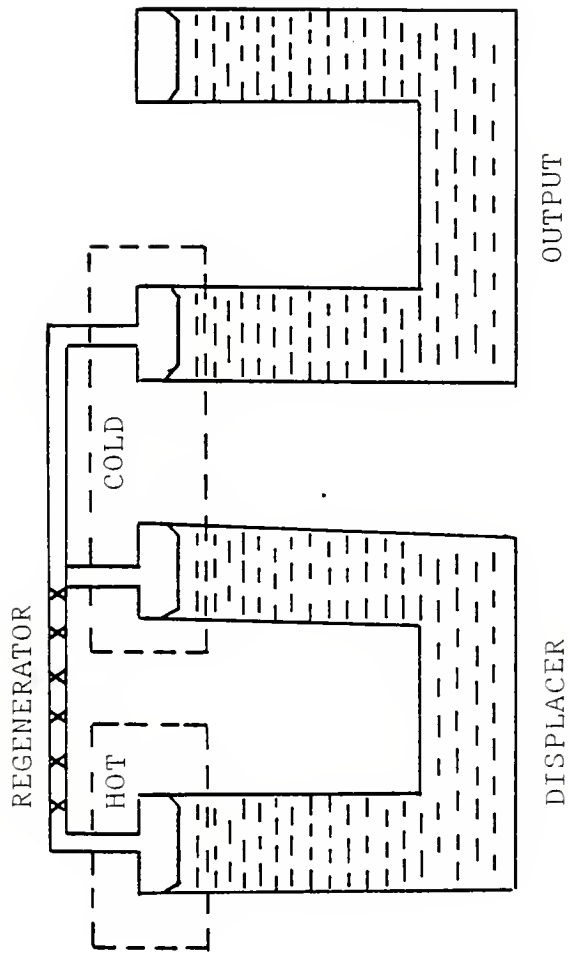Figure 1. Thermodynamic representation of the Stirling cycle.
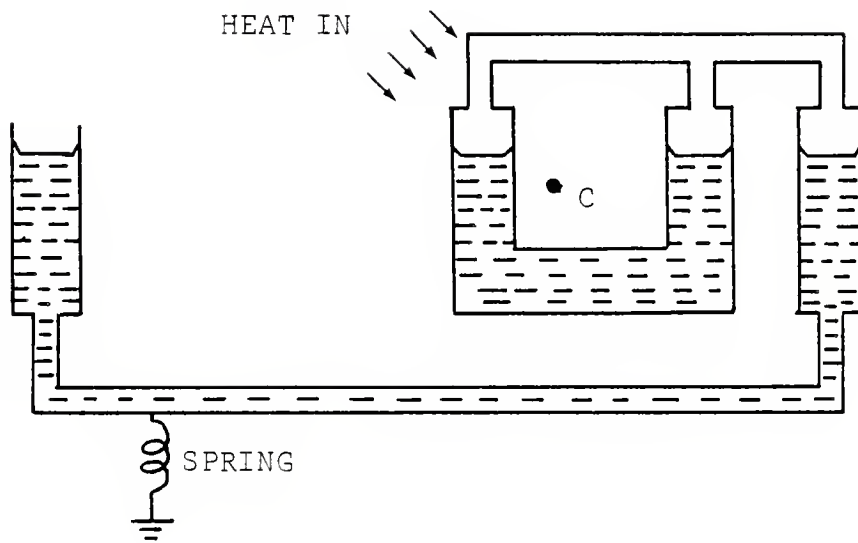
Figure 2. The basic Fluidyne.

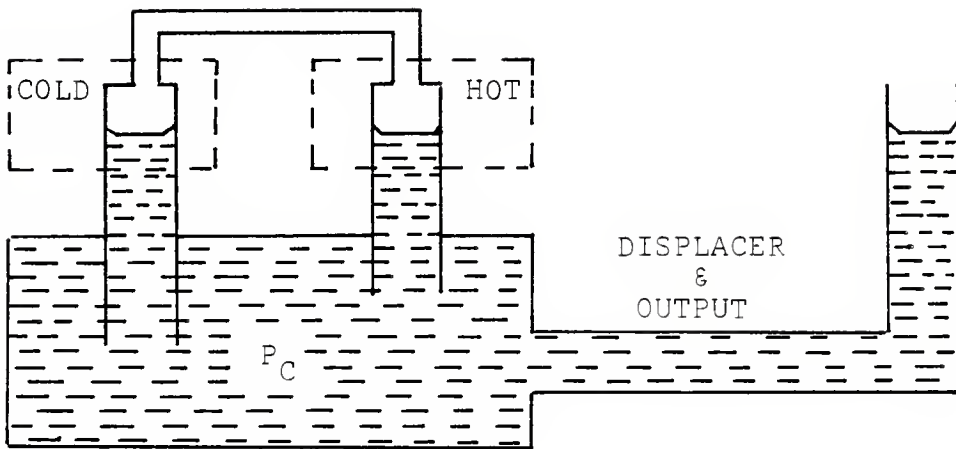Figure 3. The Fluidyne with rocking
beam feedback.

Figure 4.   The Fluidyne in a pressure
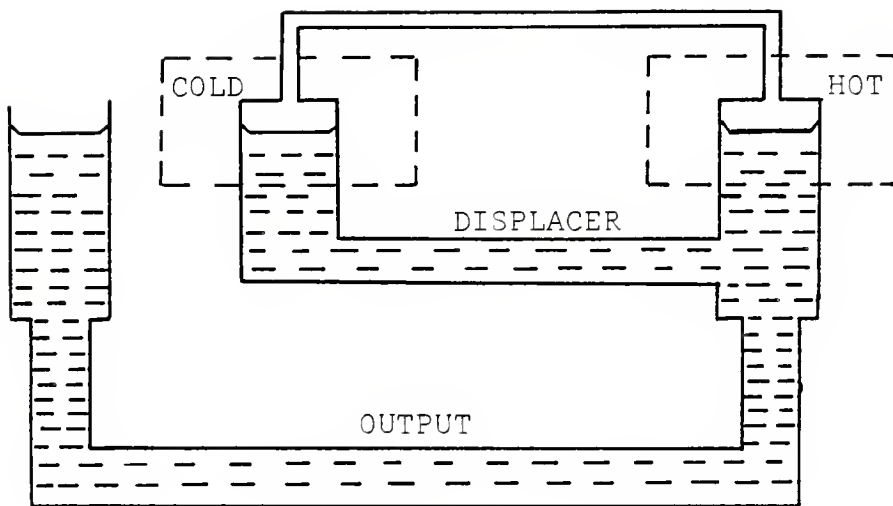   feedback configuration.

Figure 5. The Fluidyne in a jet-stream
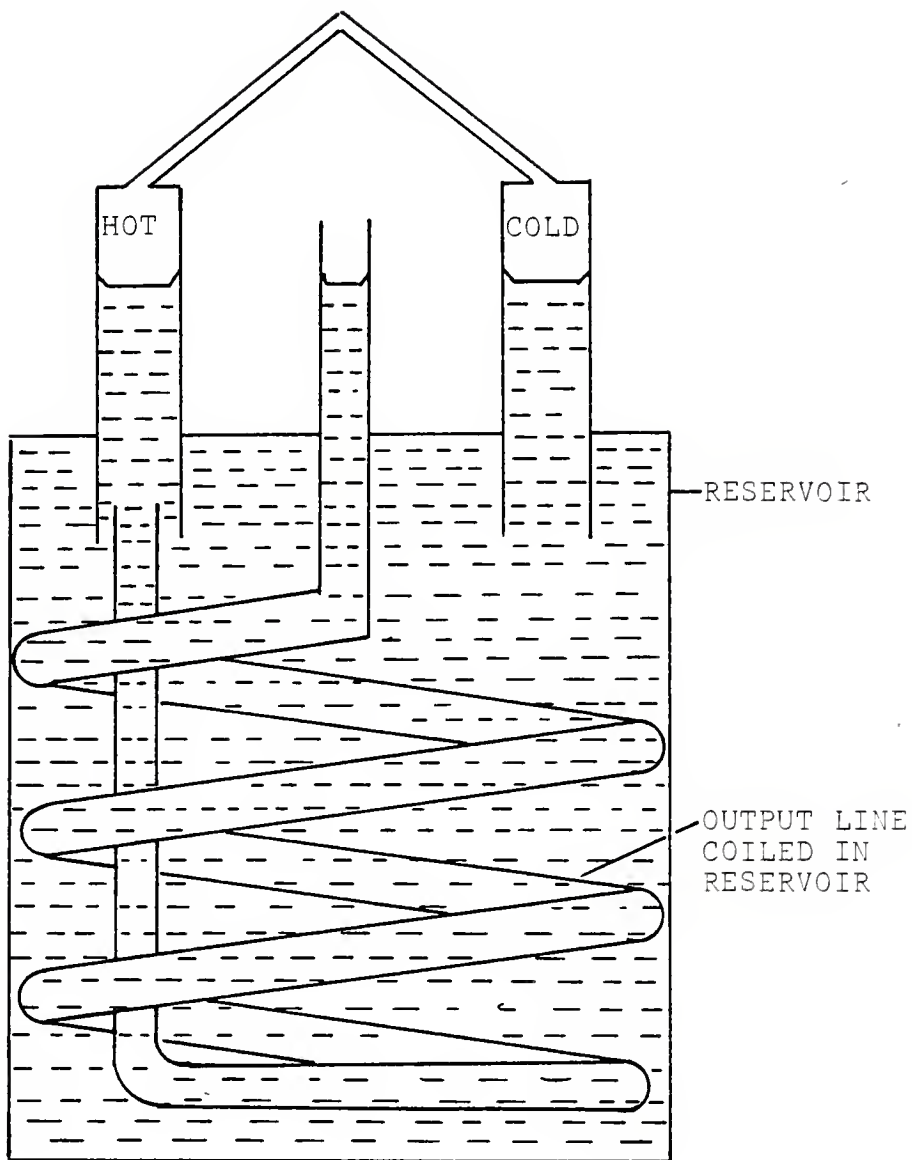feedback configuration.

Figure 6. Alternative configuration
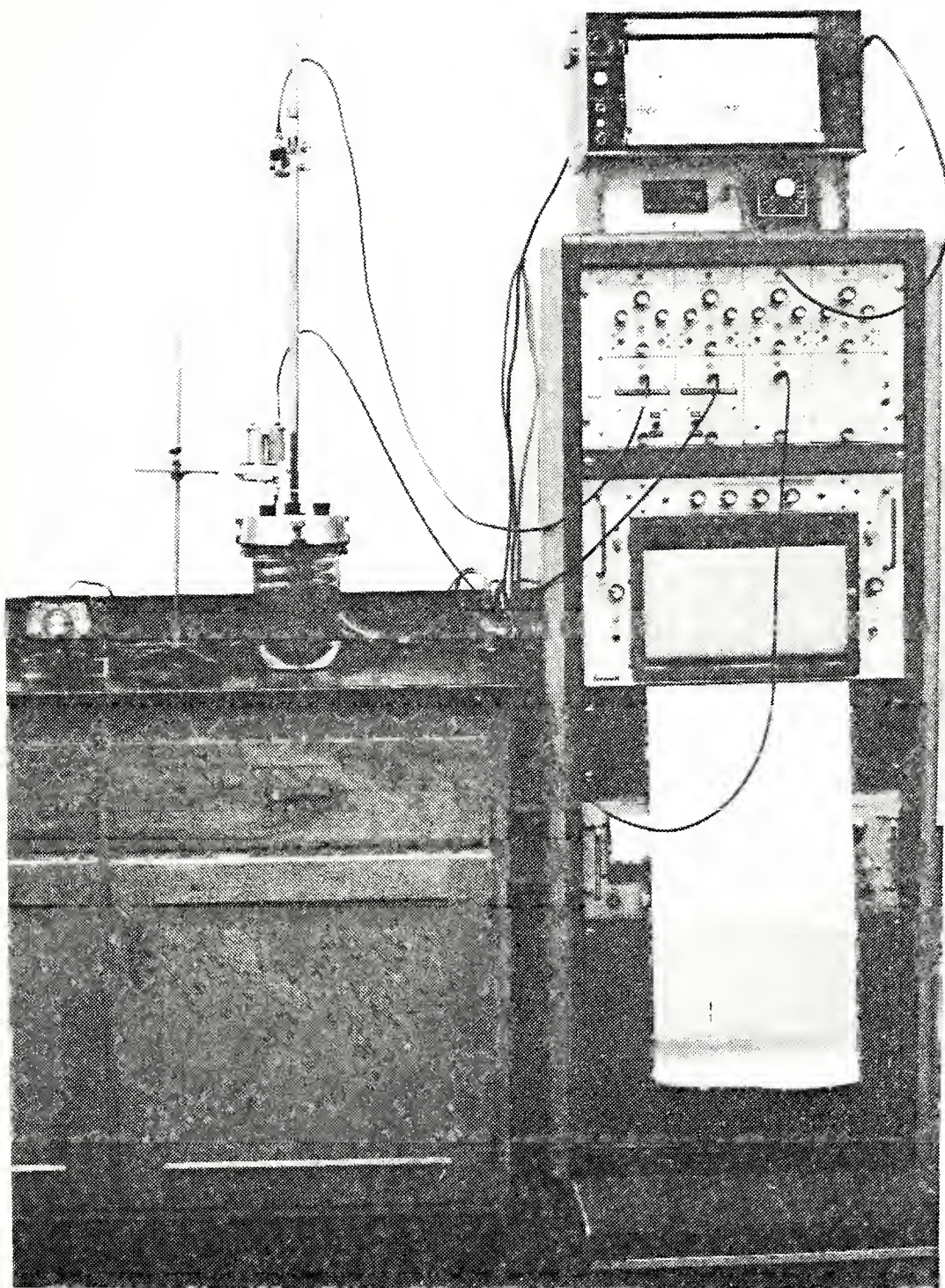for jet-stream feedback.

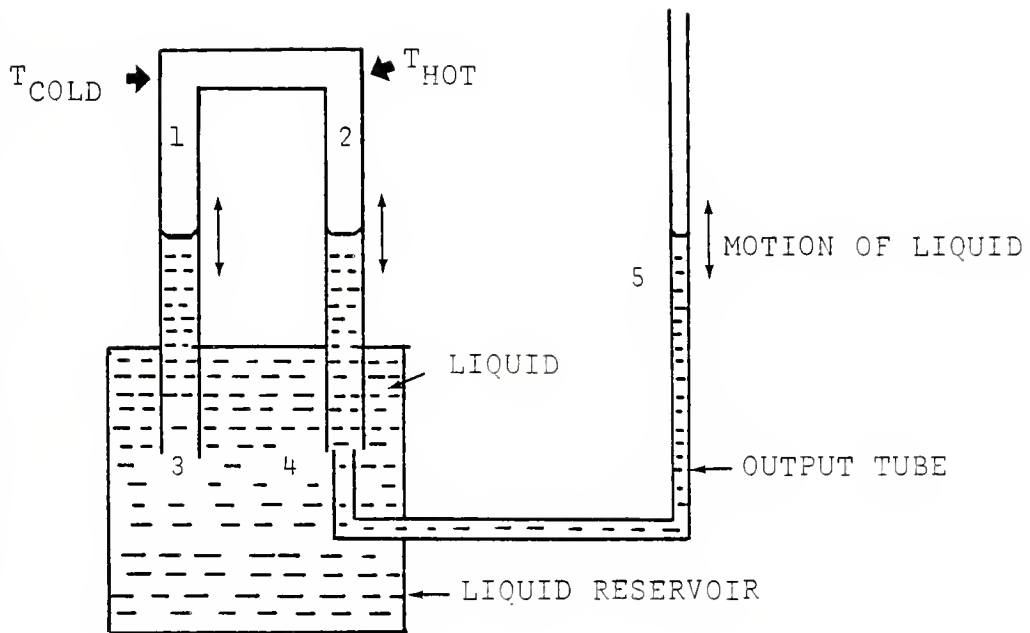Figure 7. Photograph of Fluidyne test facility.

Figure 8. Schematic of a Fluidyne pump.
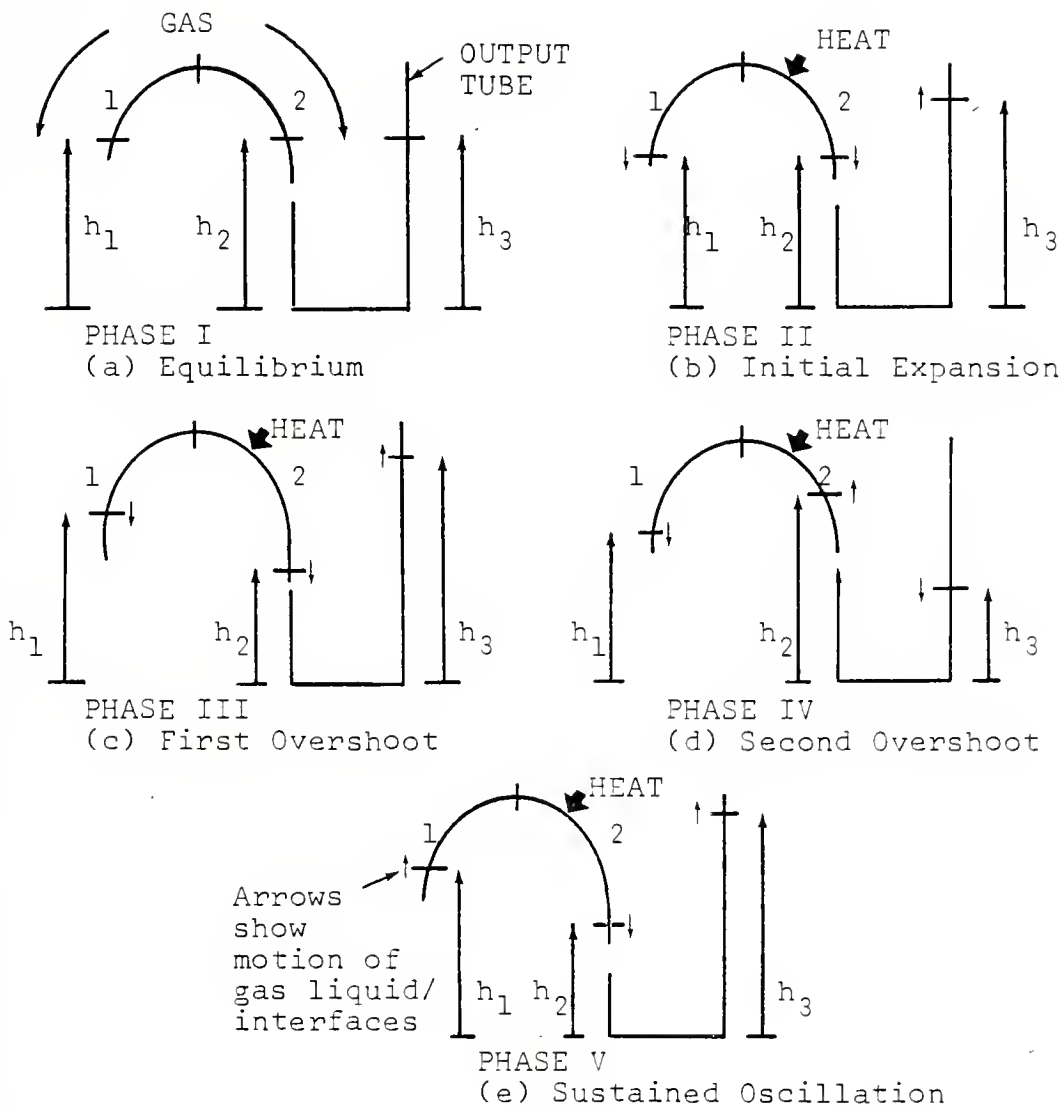
Figure 9.   Schematic representation of Fluidyne
            start-up process.
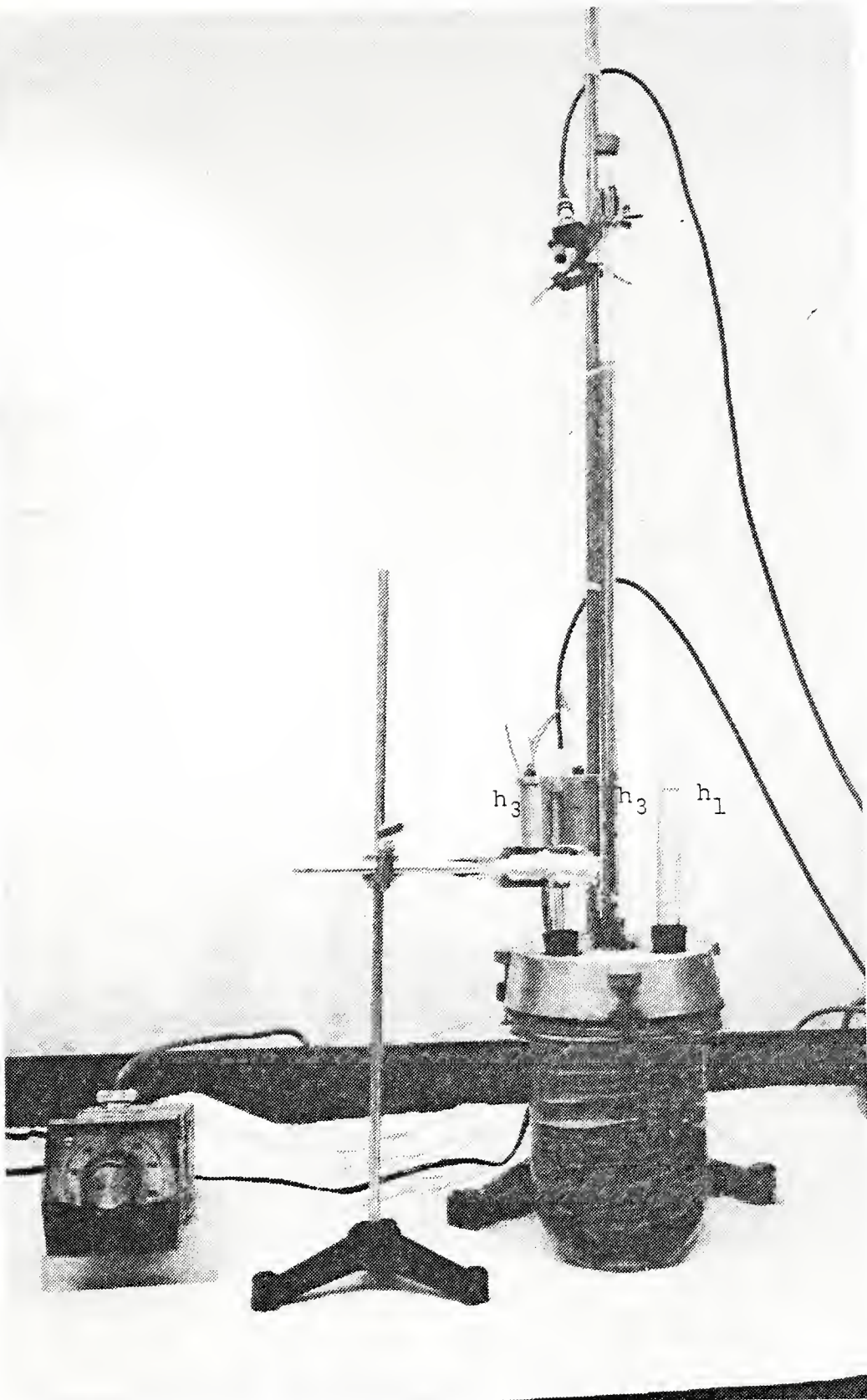
Figure 10.   Photograph of Fluidyne depicting Phase I.
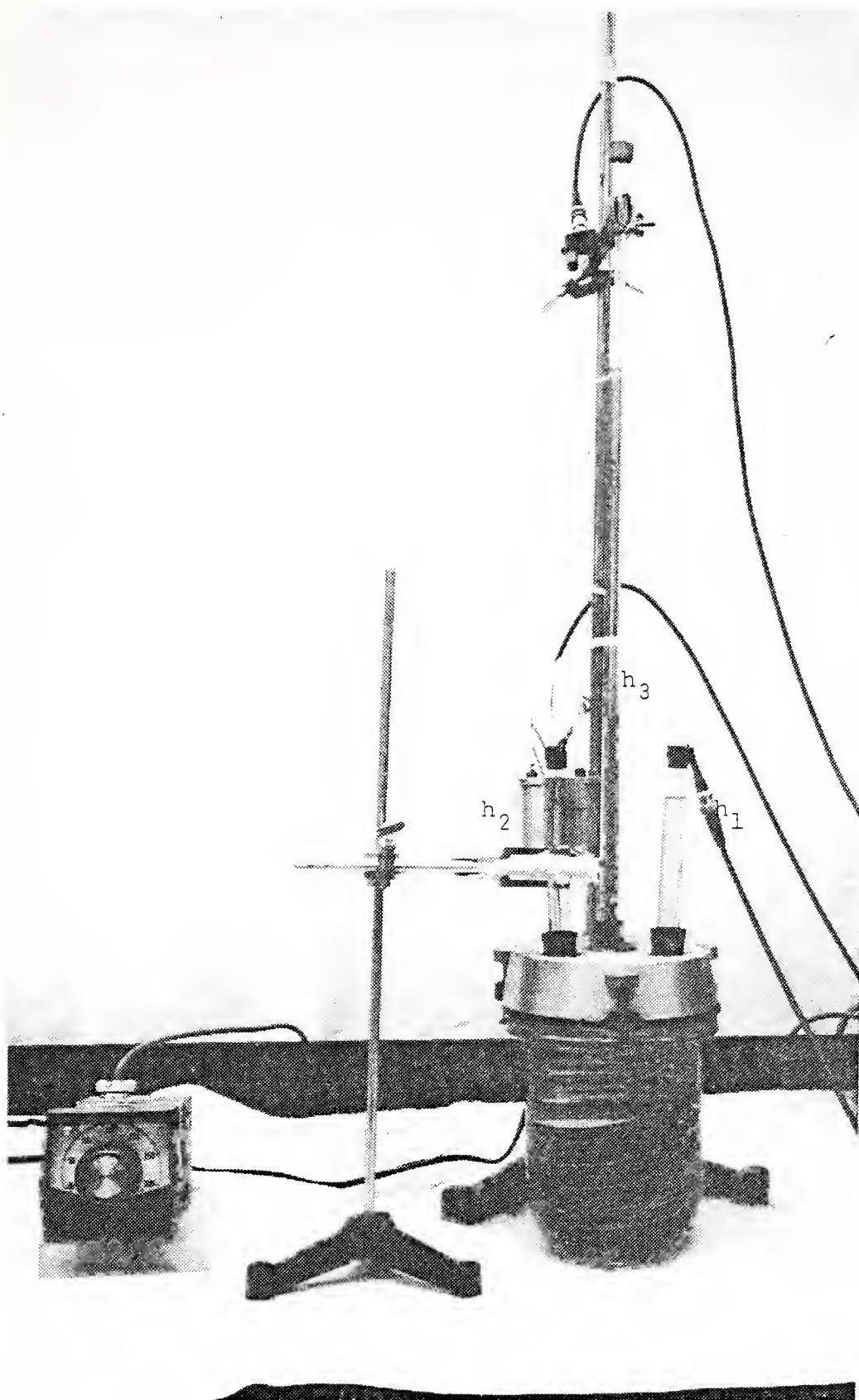
Figure 11. Photograph of Fluidyne depicting Phase II.
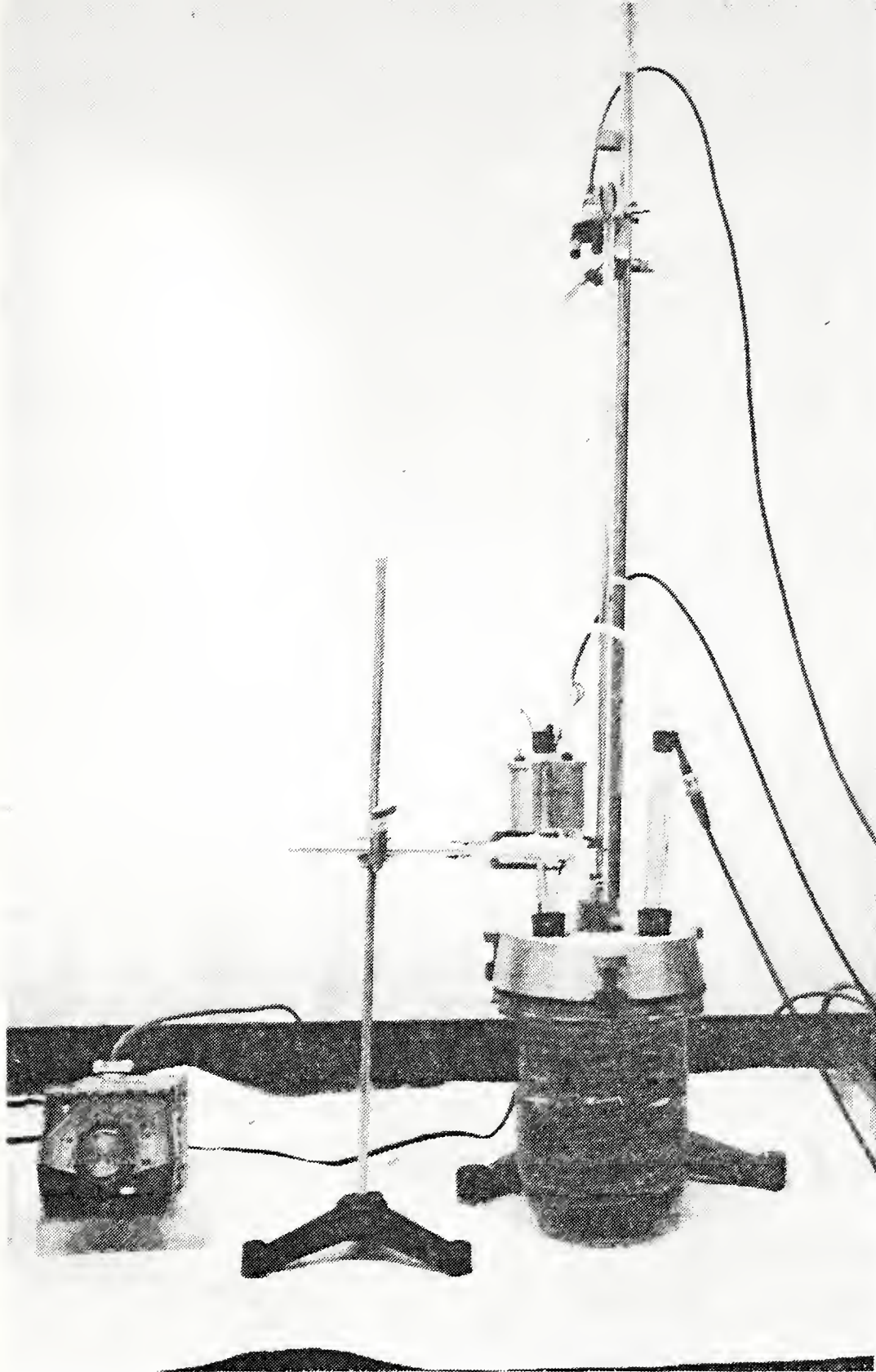
Figure 12. Photograph of Fluidyne depicting
Phases III, IV, and V.
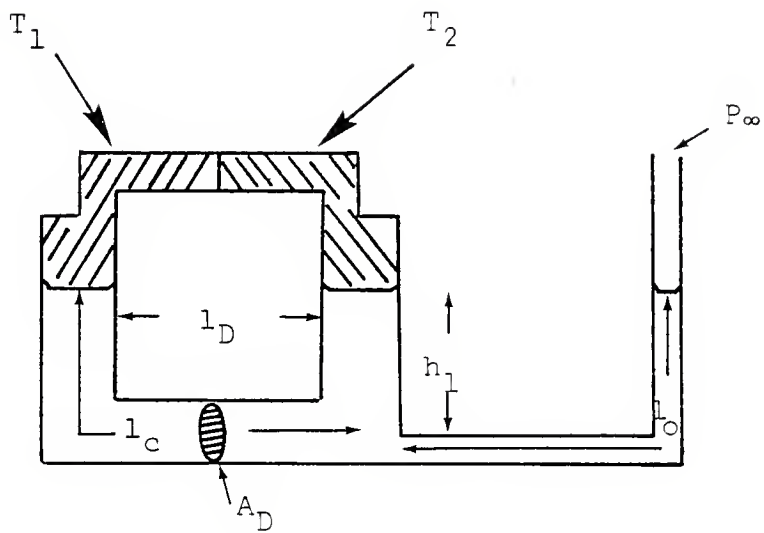
Figure 13.   Schematic of Fluidyne
used by Geisow [3].

FLUIDYNE 3
PUMP
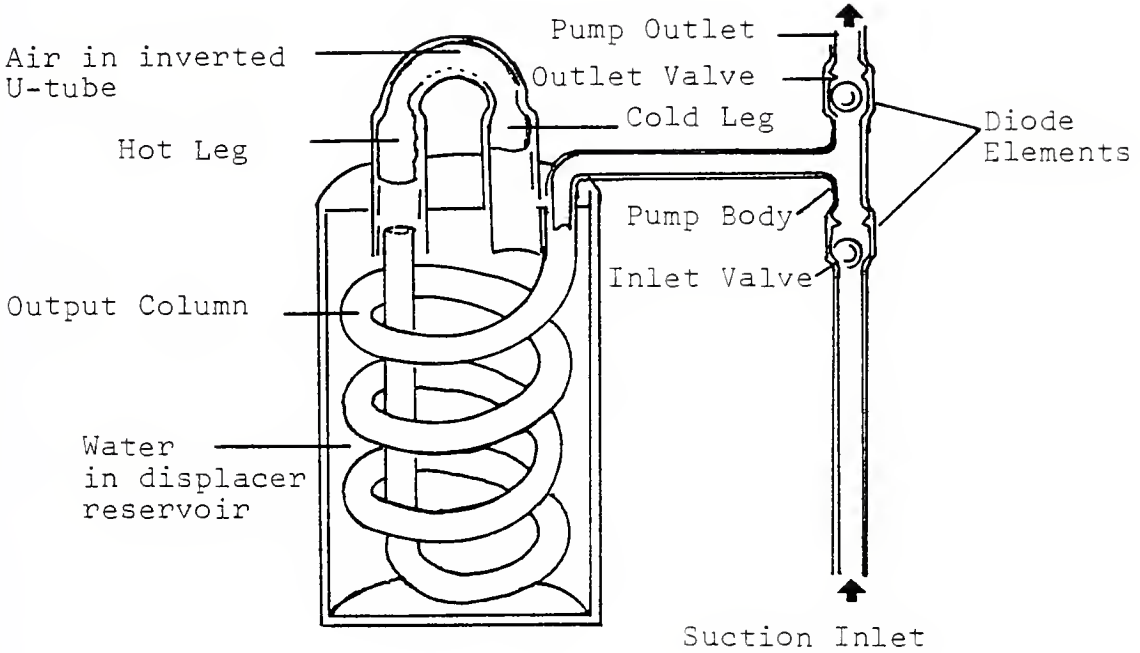
Figure 14. Schematic of an actual
            Fluidyne pump.
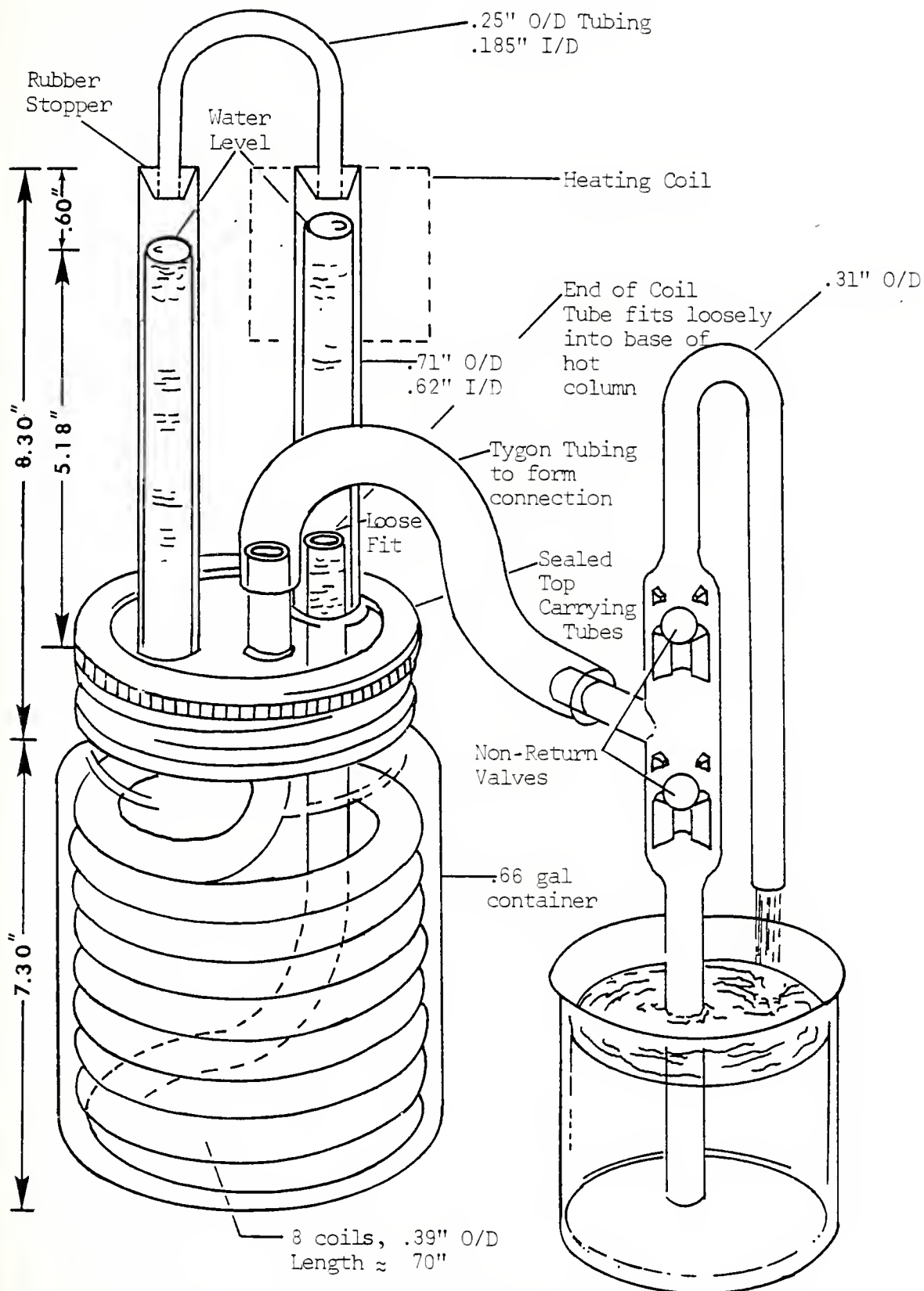
Figure 15. Schematic of actual Fluidyne assembly used in experiments.
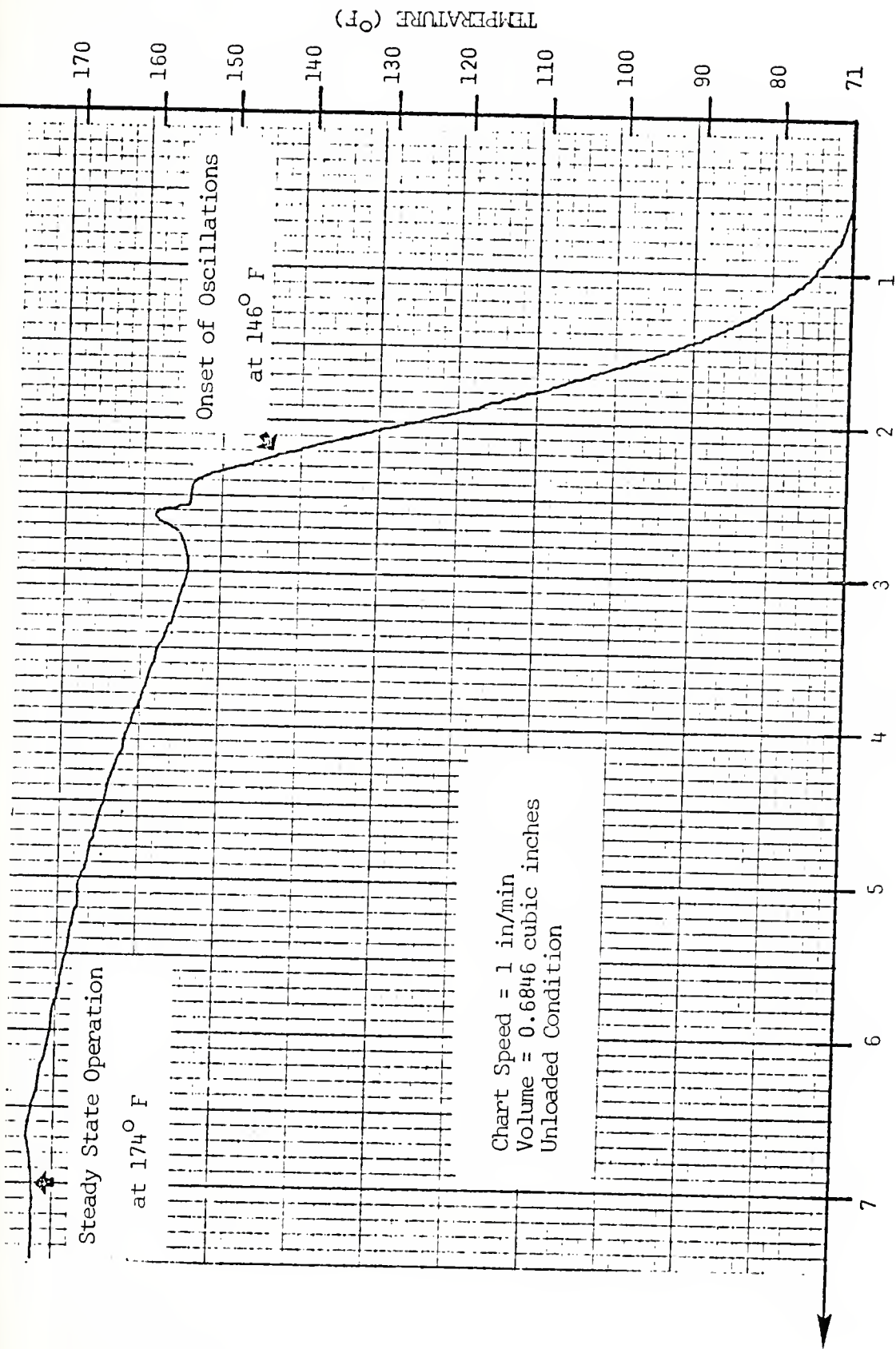
Figure 16. Strip chart recorder output - gas temperature vs time,
Volume = 0.6846 cubic inches.

62
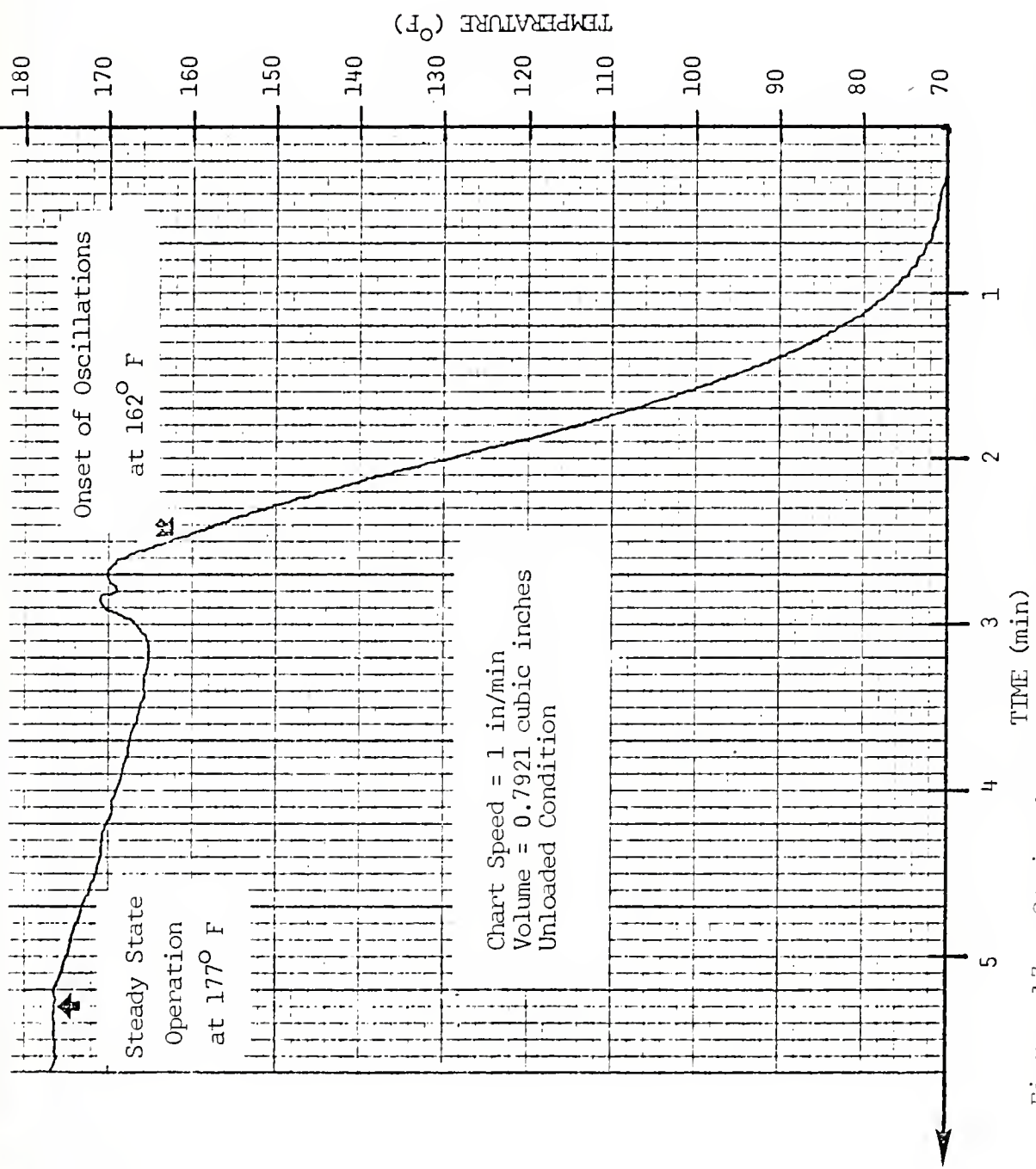
Figure 17. Strip chart recorder output - gas temperature vs time, Volume = 0.7921 cubic inches.
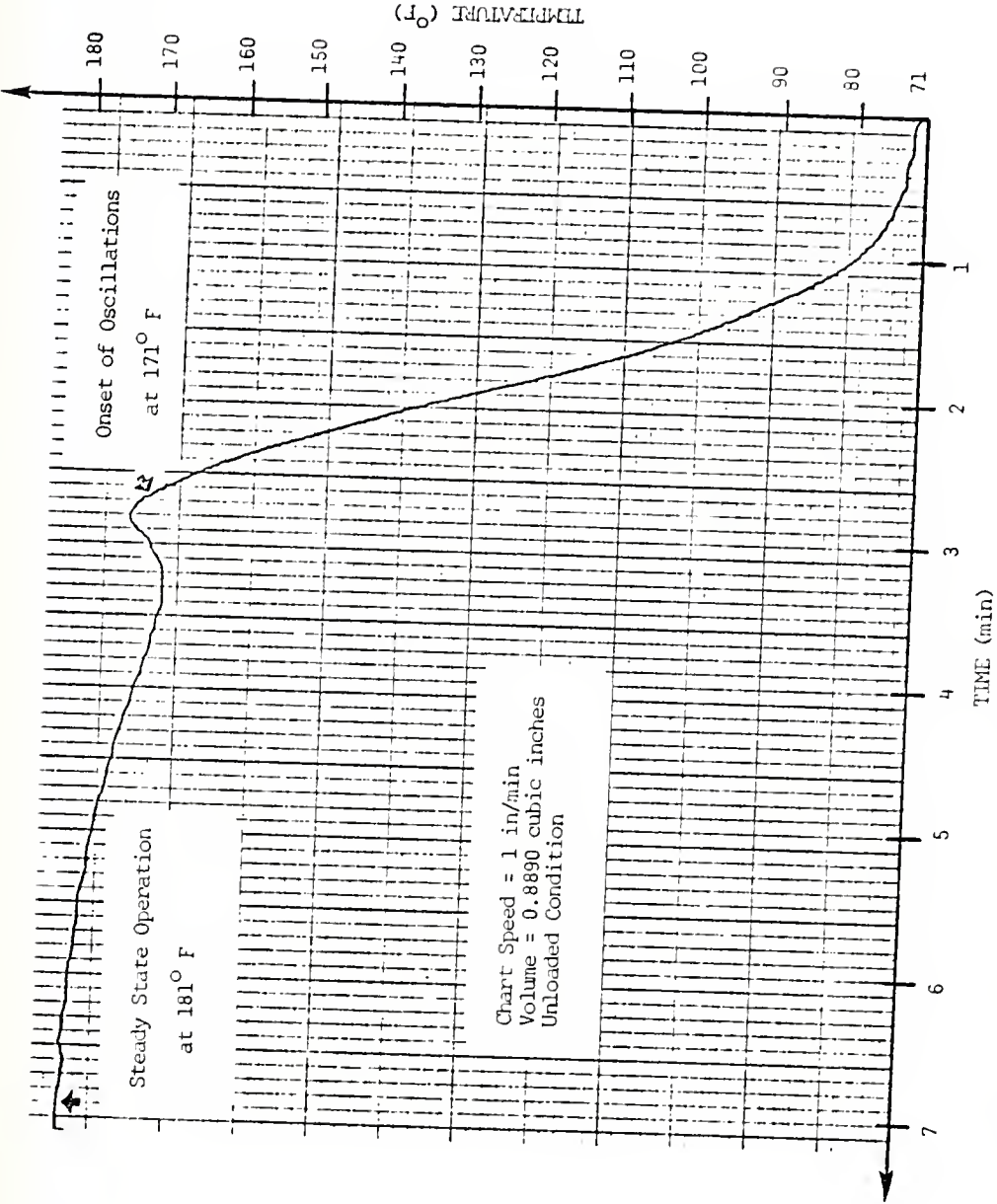
Figure 18. Strip chart recorder output - gas temperature vs time, Volume = 0.8890 cubic inches.

64
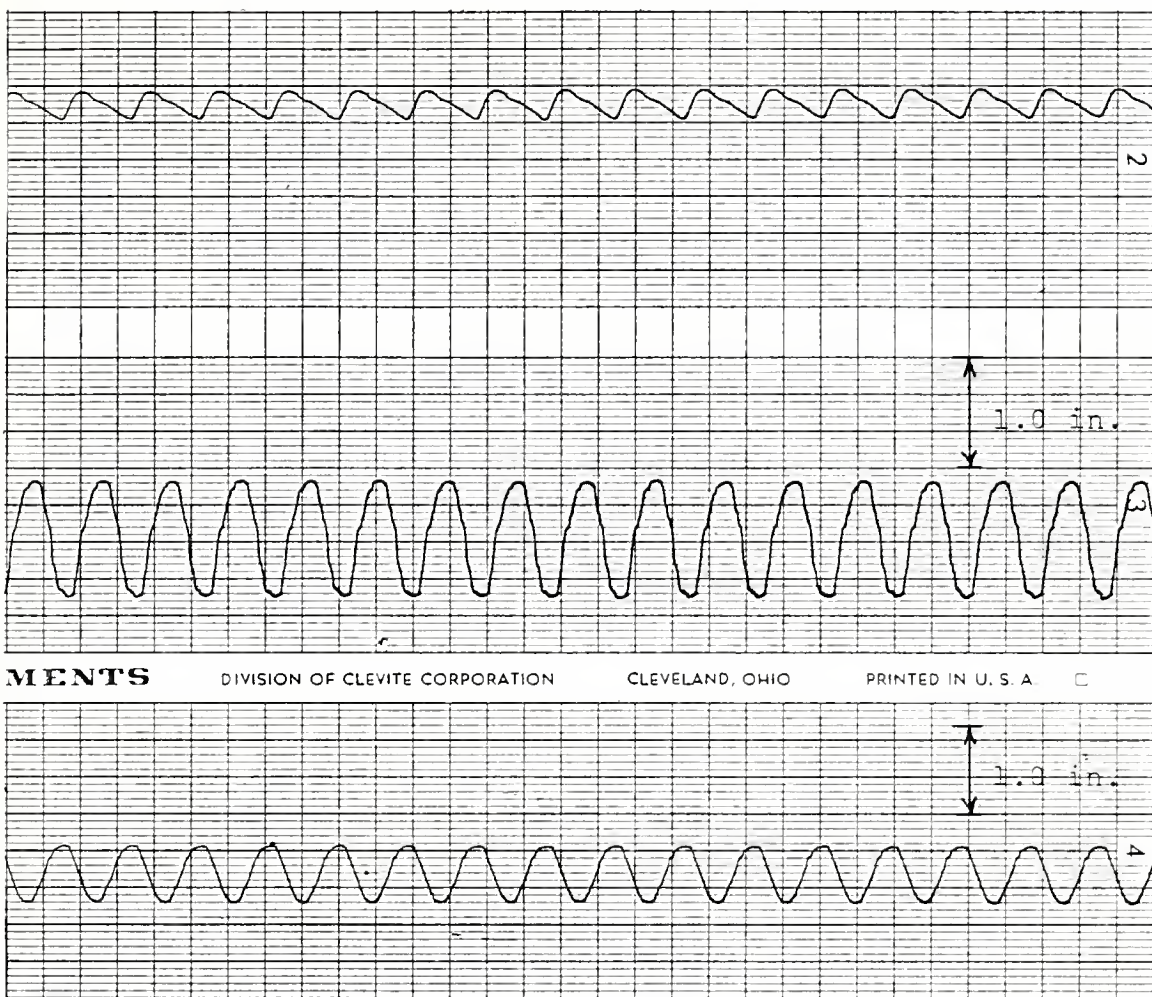
MENTS   DIVISION OF CLEVITE CORPORATION   CLEVELAND, OHIO   PRINTED IN U. S. A.

RUN CHARACTERISTICS:

Total Volume = 0.5233 cu in.
Temperature = 161°F
Chart Speed = 10 mm/sec

READ GRAPHS TOP TO BOTTOM:

Output Column
Hot Column
Cold Column

SCALES:

Output Column   Not Calibrated
Hot Column   15 lines = 1 in.
Cold Column   12 lines = 1 in.

Figure 19.   Oscillograph output - liquid column levels,
              Volume = 0.5233 cubic inches.
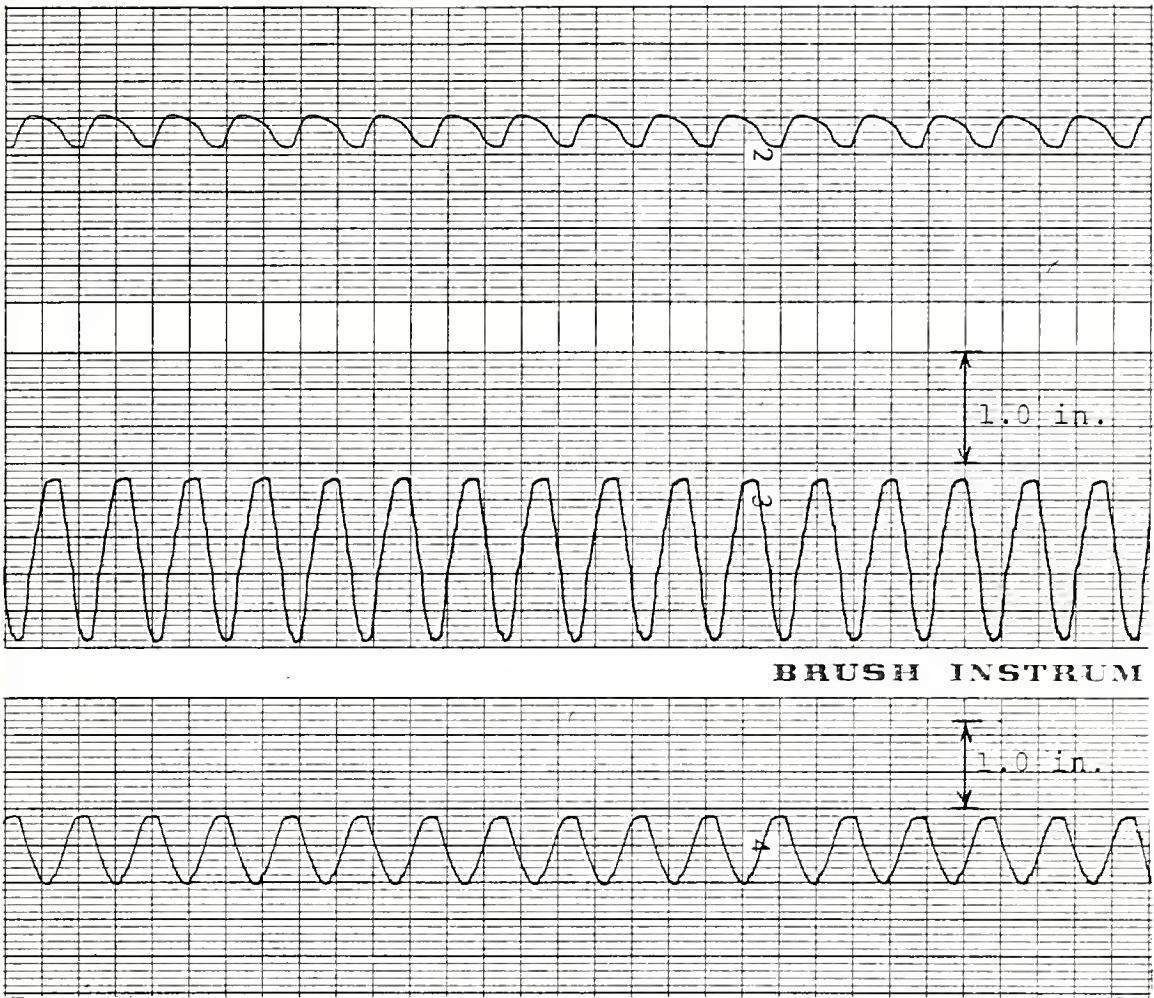
RUN CHARACTERISTICS:

Total Volume = 0.6848 cu in.
Temperature = 159°F
Chart Speed = 10 mm/sec
Unloaded Condition

READ GRAPHS TOP TO BOTTOM:

Output Column
Hot Column
Cold Column

SCALES:

Output Column	Not Calibrated
Hot Column	15 lines = 1 in.
Cold Column	12 lines = 1 in.

Figure 20.   Oscillograph output - liquid column levels,
             Volume = 0.6848 cubic inches.

RUN CHARACTERISTICS: READ GRAPHS TOP TO BOTTOM:

Total Volume = 0.8458 cu in.   Output Column
Temperature = 161°F   Hot Column
Chart Speed = 10 mm/sec   Cold Column
Unloaded Condition

SCALES:

Output Column   Not Calibrated
Hot Column   15 lines = 1 in.
Cold Column   12 lines = 1 in.

Figure 21.   Oscillograph output - liquid column levels,
             Volume = 0.8458 cubic inches.

67
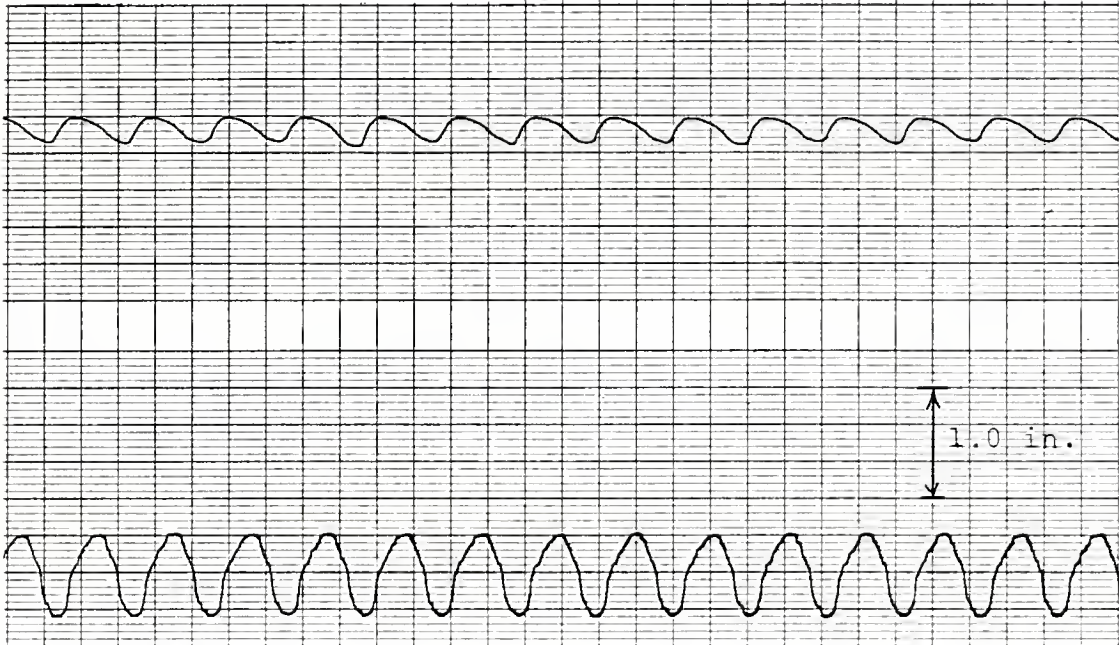
STRUMENTS DIVISION OF CLEVITE CORPORATION CLEVELAND, OHIO PRINTED IN U. S
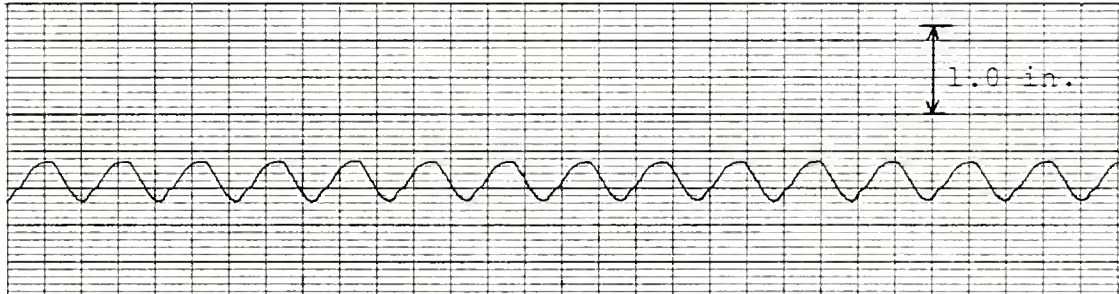
RUN CHARACTERISTICS:

Total Volume = 1.329 cu in.
Temperature = 185°F
Chart Speed = 10 mm/sec
Unloaded Condition

READ GRAPHS TOP TO BOTTOM:

Output Column
Hot Column
Cold Column

SCALES:

Output Column	Not Calibrated
Hot Column	15 lines = 1 in.
Cold Column	12 lines = 1 in.

Figure 22. Oscillograph output - liquid column levels,
Volume = 1.329 cubic inches.

68
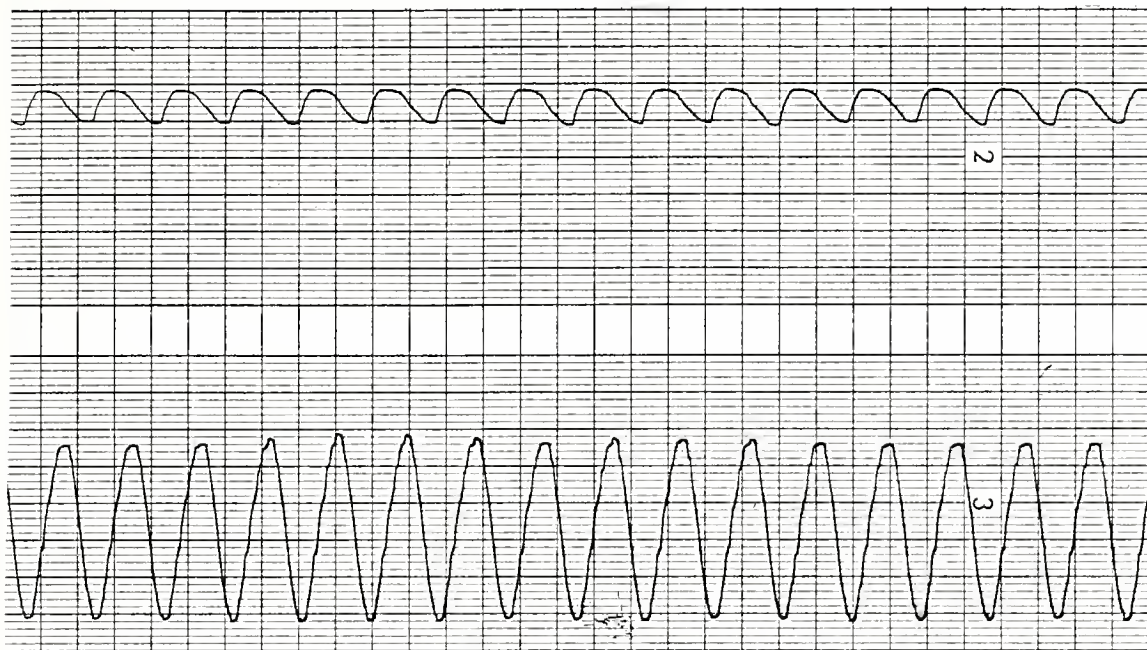
BRUSH
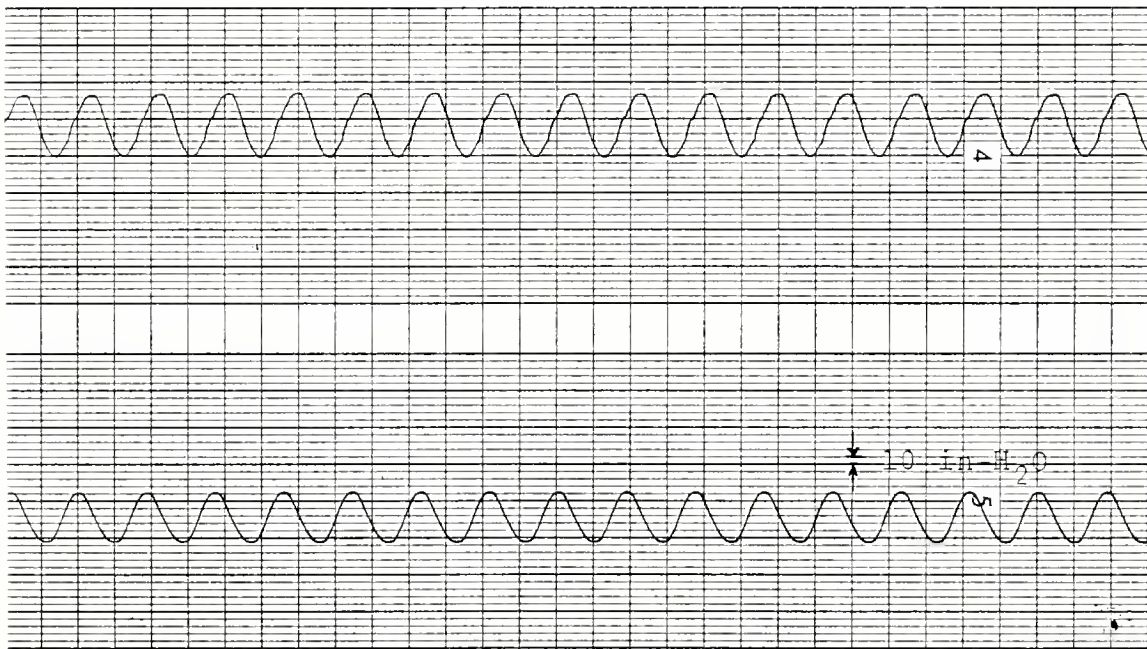
RUN CHARACTERISTICS: READ GRAPHS TOP TO BOTTOM:
Total Volume = 0.8345 cu in.   Output Column
Temperature = 164°F   Cold Column
Chart Speed = 10 mm/sec   Hot Column
Unloaded Condition   Gas Pressure

SCALES:
Gas Pressure   1 line = 10 in-H_2O
Others Not Calibrated

Figure 23.   Oscillograph output - liquid column
levels and gas pressure.
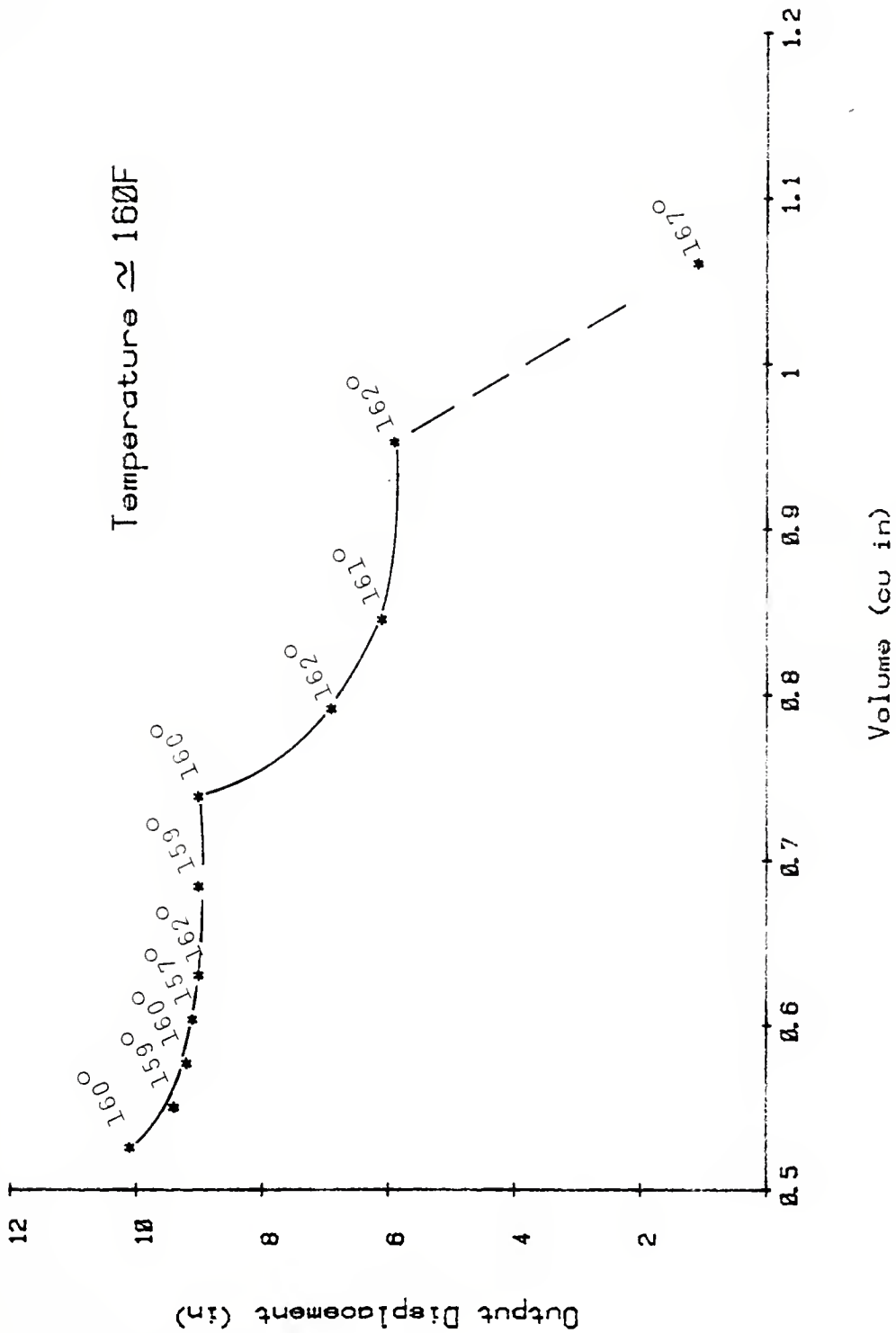
Figure 24. Volume vs output displacement at a constant temperature.
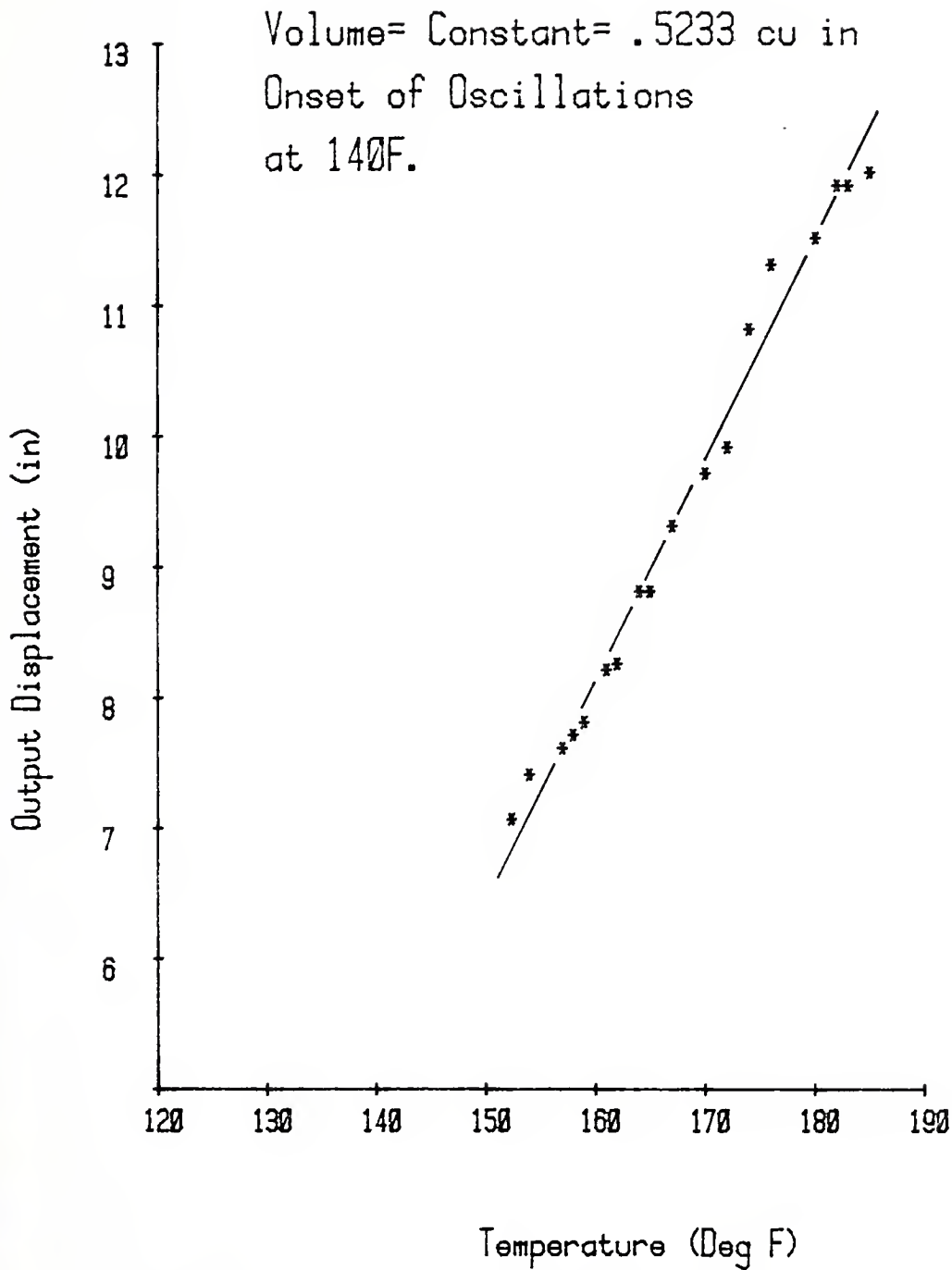
Figure 25.   Temperature vs output displacement.
           Volume = 0.5233 cubic inches.
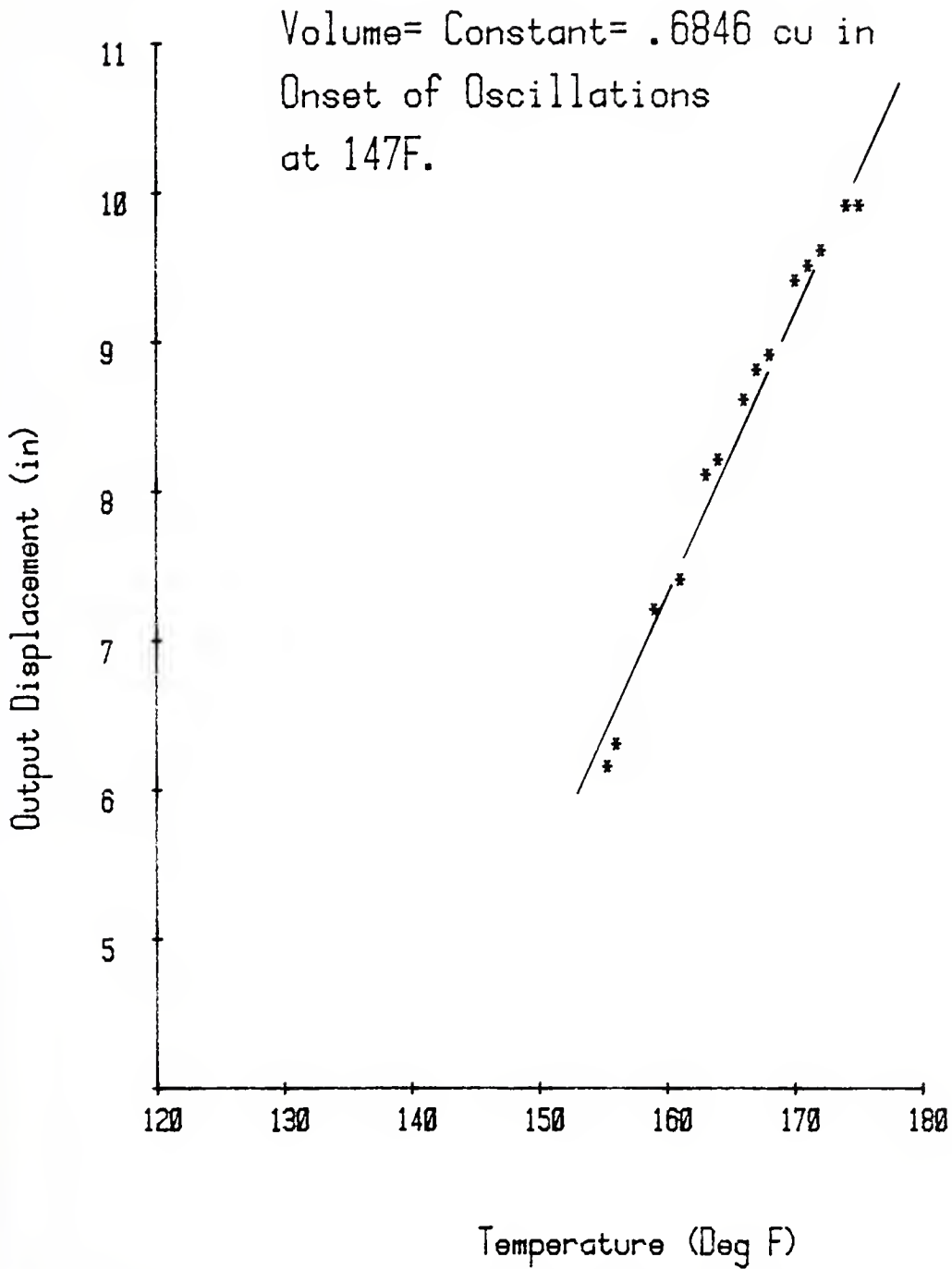
Figure 26. Temperature vs output displacement.
Volume = 0.6846 cubic inches.
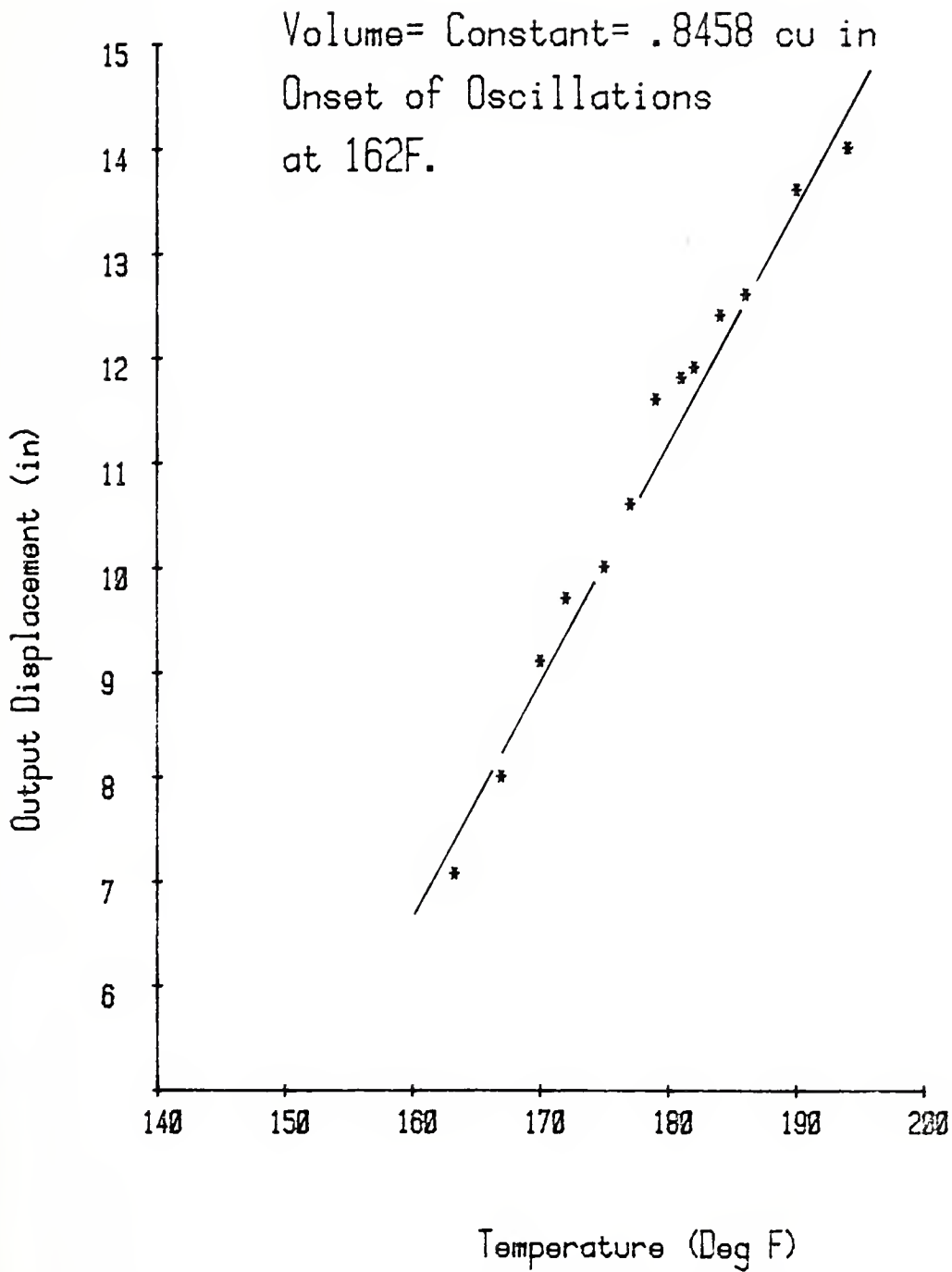
Figure 27.   Temperature vs output displacement.
             Volume = 0.8458 cubic inches.
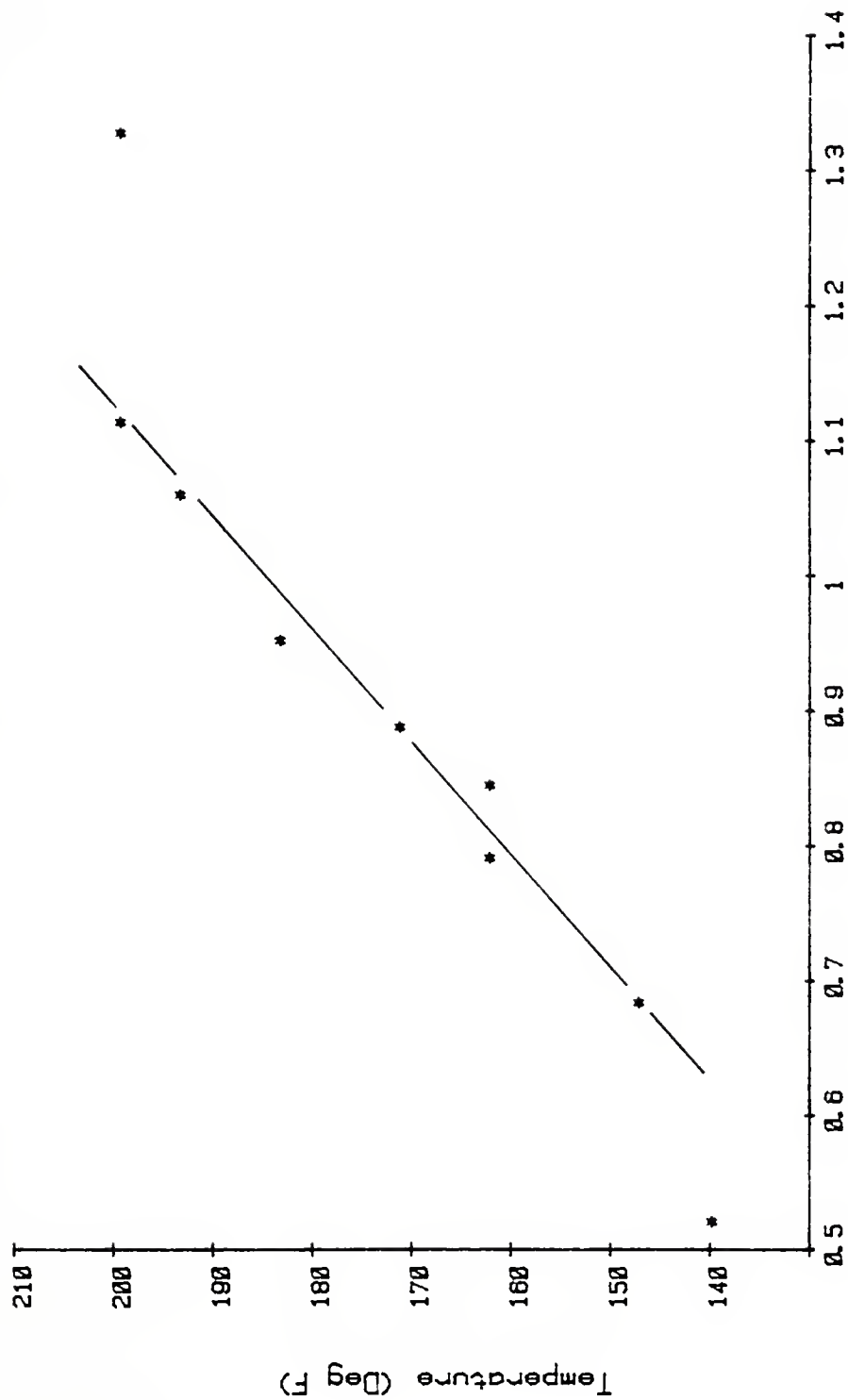
Figure 28. Temperature required for the onset of oscillations.

TOTAL VOLUME (cu in.)	HOT GAS TEMP. (°F)	HOT COLUMN FREQ. (Hz)	COLD COLUMN FREQ. (Hz)	OUTPUT COLUMN FREQ. (Hz)	HOT COLUMN PERIOD (sec)	COLD COLUMN PERIOD (sec)	OUTPUT COLUMN PERIOD (sec)
0.5233	161	1.020	1.020	1.020	0.9804	0.9804	0.9804
0.6846	159	1.020	1.020	1.020	0.9804	0.9804	0.9804
0.8458	161	1.020	1.020	1.020	0.9804	0.9804	0.9804
1.329	185	0.9259	0.9259	0.9259	1.08	1.08	1.08

Table I. Frequency and period results.

75

TOTAL VOLUME (cu in.)	HOT GAS TEMPERATURE (^{o}F)	HOT COLUMN OUT OF PHASE WITH COLD COLUMN (degrees)	OUTPUT COLUMN OUT OF PHASE WITH COLD COLUMN (degrees)
0.5233	161	187.2	88.13
0.6846	159	201.96	121.18
0.8458	161	216.65	128.52
1.329	185	236.0	163.33

Table II.   Phase angle comparison with cold
column in unloaded condition.

GAS VOLUME (cu in.)	GAS TEMPERATURE AT START (°F)	GAS TEMPERATURE AT FINISH (°F)	ELAPSED TIME (sec)	AMOUNT PUMPED (ml)	PUMPING HEAD AT START (in)	PUMPING HEAD AT FINISH (in)	FLOW RATE GAL/MIN
0.6308	162	163	66.4	250	9.6	10.2	0.05968
	163	164	64.4	250	10.2	10.8	0.06154
	164	164	72.0	250	10.8	11.4	0.05504
	165	167	75.0	250	11.4	12.0	0.05284
	167	168	80	240	12.0	12.6	0.04756

Table III. Performance characteristics of the Fluidyne heat engine in the loaded configuration, gas temperature 162-168°F.

GAS VOLUME (cu in.)	GAS TEMPERATURE AT START (^{o}F)	GAS TEMPERATURE AT FINISH (^{o}F)	ELAPSED TIME (sec)	AMOUNT PUMPED (ml)	PUMPING HEAD AT START (in)	PUMPING HEAD AT FINISH (in)	FLOW RATE GAL/MIN
0.6308	171	170	55	250	9.6	10.2	0.0721
	170	171	48	250	10.2	10.8	0.0826
	171	173	56	250	10.8	11.4	0.0708
	173	175	57	250	11.4	12.0	0.0695
	175	177	59	250	12.0	12.6	0.0672
	177	181	71	250	12.6	13.2	0.0558
	181	183	71	250	13.2	13.8	0.0558
	183	182	72	250	13.8	14.4	0.0550

Table IV. Performance characteristics of the Fluidyne heat engine in the loaded configuration, gas temperature 171-182°F.

GAS VOLUME (cu in.)	GAS TEMPERATURE AT START (°F)	GAS TEMPERATURE AT FINISH (°F)	ELAPSED TIME (sec)	AMOUNT PUMPED (ml)	PUMPING HEAD AT START (in)	PUMPING HEAD AT FINISH (in)	FLOW RATE GAL/MIN
0.6308	175	167	40.6	250	9.6	10.2	0.0976
	167	166	46.2	250	10.2	10.8	0.0858
	166	167	45.2	250	10.8	11.4	0.0877
	167	168	53.0	250	11.4	12.0	0.0748
	168	169	48.0	250	12.0	12.6	0.0826
	169	170	54.0	250	12.6	13.2	0.0734
	170	173	52.2	250	13.2	13.8	0.0759
	173	175	60	250	13.8	14.4	0.0661

Table V. Performance characteristics of the Fluidyne heat engine in the loaded configuration, gas temperature 175°F.

TOTAL VOLUME (cu in.)	TEMPERATURE REQUIRED FOR ONSET OF OSCILLATIONS ($^{\circ}$F)
.5233	140
.6846	147
.7921	162
.8458	162
1.8890	171
1.9530	183
1.061	193
1.115	199
1.329	199

Table VI. Temperature necessary for the onset of oscillations in the unloaded condition.

TOTAL VOLUME (cu in.)	HOT GAS TEMPERATURE ($^{\circ}$F)	OUTPUT COLUMN DISPLACEMENT (in)
0.5233	161	10.0
0.5502	159	9.4
0.5770	160	9.2
0.6039	157	9.1
0.6308	162	9.0
0.6846	159	9.0
0.7386	160	9.0
0.7921	162	6.9
0.8458	161	6.1
0.9530	162	5.9
1.061	167	1.1

Table VII. Output displacement results
at a constant temperature.

TOTAL VOLUME (cu in.)	HOT GAS TEMP. (°F)	HOT COLUMN FREQUENCY (Hz)	COLD COLUMN FREQUENCY (Hz)	OUTPUT COLUMN FREQUENCY (Hz)	HOT COLUMN DISPLACEMENT (in)	COLD COLUMN DISPLACEMENT (in)	OUTPUT COLUMN DISPLACEMENT (in)
0.5233	161	1.020	1.020	1.020	1.02	0.6417	10.0
0.6846	159	1.020	1.020	1.020	1.447	0.7416	9.0
0.8458	161	1.020	1.020	1.020	0.9333	0.4917	6.1
1.329	185	0.9259	0.9259	0.9259	0.7333	0.4333	7.8

Table VIII.   Summary of displacement levels and frequency in the unloaded configuration.

82

VOLUME (cu in.)	TEMPERATURE ($^{\circ}$F)	MAXIMUM AMPLITUDE (in)	MINIMUM AMPLITUDE (in)	OUTPUT AMPLITUDE (in)
0.5233	152	10.2	3.2	7.0
	154	10.5	3.1	7.4
	157	10.7	3.1	7.6
	158	10.9	3.2	7.7
	159	11.0	3.2	7.8
	161	11.3	3.1	8.2
	162	11.45	3.2	8.25
	164	11.9	3.1	8.8
	165	12.0	3.2	8.8
	167	12.4	3.1	9.3
	170	12.9	3.2	9.7
	172	13.2	3.3	9.9
	174	13.7	2.9	10.8
	176	14.4	3.1	11.3
	180	14.6	3.1	11.5
	182	15.3	3.4	11.9
	183	15.7	3.8	11.9
	185	15.9	3.9	12.0

Note: No values were obtained beyond 185°F due to saturation of the connecting gas tube volume.

Table IX. Visual output displacement data, Volume = 0.5233 cubic inches.

VOLUME (cu in.)	TEMPERATURE (°F)	MAXIMUM AMPLITUDE (in)	MINIMUM AMPLITUDE (in)	OUTPUT AMPLITUDE (in)
0.6846	155	8.4	2.3	6.1
	156	8.5	2.2	6.3
	159	9.1	1.9	7.2
	161	9.3	1.9	7.4
	163	9.8	1.7	8.1
	164	9.9	1.7	8.2
	166	10.2	1.6	8.6
	167	10.4	1.6	8.8
	168	10.5	1.6	8.9
	170	10.9	1.5	9.4
	171	11.1	1.6	9.5
	172	11.2	1.6	9.6
	174	11.5	1.6	9.9
	175	11.6	1.7	9.9

Note: No values were obtained beyond 175°F due to saturation of the connecting gas tube volume.

Table X. Visual output displacement data, Volume = 0.6846 cubic inches.

VOLUME (cu in.)	TEMPERATURE (°F)	MAXIMUM AMPLITUDE (in)	MINIMUM AMPLITUDE (in)	OUTPUT AMPLITUDE (in)
0.8458	163	11.6	4.6	7.0
	167	12.4	4.4	8.0
	170	13.2	4.1	9.1
	172	13.7	4.0	9.7
	175	14.0	4.0	10.0
	177	14.6	4.0	10.6
	179	15.4	3.8	11.6
	181	15.7	3.9	11.8
	182	15.8	3.9	11.9
	184	16.3	3.9	12.4
	186	16.6	4.0	12.6
	190	17.8	4.2	13.6
	194	18.0	4.0	14.0

Note: No values were obtained beyond 194°F due to controller setting at maximum limit.

Table XI.   Visual output displacement data, Volume = 0.8458 cubic inches.

APPENDIX A

UNCERTAINTY ANALYSIS

Since all experimental results were directly obtainable without the assistance of any empirical relationships, the uncertainty associated with this experimental work is limited primarily to that of the instrumentation and the error introduced in the direct recording of readings.

The following are considered to be representative uncertainties in the recording of this data.

Variable	Uncertainty
T_h , T_c	$\pm$ 1°F
h_e	$\pm$ .125 in.
h (pumping head)	$\pm$ .125 in.
l_c , l_h	$\pm$ .0625 in.
l_o (length of output leg)	$\pm$ 1 in.
P_g	$\pm$ .2 in-water
t (time)	$\pm$ 2 seconds
ω	$\pm$ .1 Hz
A_o (output amplitude)	$\pm$ .25 in.
V_g	$\pm$ .05 cu in.
X_c , X_h , X_o (area of columns)	$\pm$ .01 in^2
A_c , A_h (hot & cold leg amplitude)	$\pm$ .05 in.

APPENDIX B

OPERATING PROCEDURES

The following steps are suggested for operating the system shown in Figure 15 in the loaded configuration.

1. Attach the wire from the controller directly to the heating coil, by allowing it to rest on the inside wall of the coil when it is fitted around the hot column.

2. Install the pump in accordance with step 10 of Appendix D.

3. Insure system is filled with water to the desired level. This can be accomplished through the hot, cold, or output column.

4. Install the connecting gas tube by inserting the ends of the tube through the openings provided in the sealing stoppers.

5. System is now ready for the heat input. A push button on the face of the controller provides this service.

6. Proper safe operating temperatures should be determined from Table VI, with the upper limit being that of boiling.

7. The system is very difficult to self-start in the loaded condition. Thus, once the temperature range for oscillations to occur has been reached, priming is necessary.

8. The following are recommended items to check when the system either terminates operation, or fails to operate.

a. Check the connecting gas tube for excessive water
    vapor.
b. Check the hot gas temperature for boiling.
c. Check for the proper amount of gas volume.
d. Check the location of the heating coil.
e. Check the sealing stoppers for a tight seal.
f. Check the seal between the reservoir and it's top.
g. Check for trapped air under the reservoir top.
h. Check for air bubbles inside the coil area.

APPENDIX C

SAMPLE CALCULATIONS

A. FREQUENCY

Equation (3) expresses the force balance for the oscil-
lating output column. According to this expression, the
output column of water, if undamped, would oscillate at a
frequency of

$$f_1 = \tfrac{1}{2}\pi(g \,/\, L_1)^{\tfrac{1}{2}} \tag{16}$$

where L_1 = length of the water in the output column.

The capacitance effect, in this case, is the hydrostatic
head which is proportional to the amplitude of oscillation.
Physical intuition, however, indicates that the effect of the
gas volume will be important as it is transmitted to the out-
put column through the action of the hot leg. The gas capaci-
tance is expressed as V_g/P_∞ and the appropriate undamped
natural frequency for the output column working against this
capacitance would be

$$f_g = \frac{1}{2\pi} \; ((P_\infty A_c / \rho \, L_1 \, V_g))^{\tfrac{1}{2}} \tag{17}$$

A = Cross sectional area of output column

V_g = Equilibrium Gas Volume

P_∞ = Equilibrium Gas Pressure

Using the following paramters,

$$L_1 = 76 \text{ in.}$$

$$P_\infty = 14.696 \text{ psia}$$

$$V_g = 0.5233 \text{ in}^3$$

$$\rho = 1.934 \text{ lb-sec}^2/\text{ft}^4$$

$$A_c = 0.03801 \text{ in}^2$$

The following results are obtained:

$$f_1 = 0.35886 \text{ Hz}$$

$$f_g = 1.9543 \text{ Hz}$$

$$f_{exper.} = 1.020 \text{ Hz, See Table I.}$$

As can be seen, the gas volume has a significant effect on the frequency behavior and the experimentally determined value lies between the two theoretical extremes. Although the circular coil diameter was 0.3937 in ID, and the extended output column section diameter 0.3150 in ID, the smaller diameter was used in the calculations above.

B. EFFICIENCY

The average power supplied to the system was estimated utilizing the following relationship.

$$P_{in} = (P_c/T_t)(t_1 + t_2 + \ldots\ldots) \tag{18}$$

where P_c = Rated power of the controller

T_t = Total time period of observation

t_1 = Time period controller is operating

The rated power of the controller was 456 watts, therefore for T_t = 449 seconds and t_1 + ... = 10 seconds, the calculated power input to this system was

$$P_{in} = 10.156 \text{ watts}$$

Utilizing data from Table V for the highest flow rate obtained,

$$P_{out} = Q \rho g h \qquad\qquad (19)$$

where h = pumping head of 9.9 inches[4]

$$P_{out} = 0.0152 \text{ watts}$$
$$\text{EFFICIENCY} = P_{out}/P_{in} = 0.149\%$$

Elrod [2] cites the following results:

Frequency = 1 Hz

Pumping Head = 2.986 ft

$$P_{in} = 250 \text{ watts}$$

$$P_{out} = 0.7145 \text{ ft-lb/sec}$$

EFFICIENCY = 0.285%

---

[4]As shown in Table V, the pumping level varied slightly during a run due to the decrease in the reservoir level. Values of h used for the calculation are the average values over the run time.

APPENDIX D

PROCEDURES FOR ASSEMBLY AND DISASSEMBLY OF THE SYSTEM

1) Install the circular coil assembly inside the reservoir
top, through the inserts provided, with some means of identifying
which end of the coil will be inserted inside the hot column
or connected to the output column. The coil ends should pro-
trude at least ½ inch above the reservoir top.

2) Fill the reservoir in which the coils are to be immersed
3/4 full of water. Install the reservoir top, with coil
assembly attached, and lock tightly with the latches provided.
High vacuum grease should be applied to the surface where the
top and reservoir make contact, to ensure a tight seal. A
poor seal will preclude operation of the system.

3) There are four openings provided in the reservoir top.
Step 2 above allows for two of these openings namely: hot and
output column. The cold column utilizes a third opening, how-
ever the fourth can be used simply as a vent. Generally, the
output column should be installed in the center as shown in
Figure 15, but not a requirement.

4) Remove the stopper in the opening to be used as the
vent, and continue filling the reservoir until completely full,
and begins to overflow onto the reservoir top.

5) Install desired length of hot and cold columns with
the aid of rubber stoppers. The output column length can be
increased by coupling onto the existing ½ inch protrusion
introduced by step 1.

92

6) Continue to fill the system with water through either of the displacement columns until the desired level is reached.

7) The heating coil should be installed at this point by fitting it around the hot column.

8) Finally, the gas tube should be inserted as shown in Figure 15.

9) The above mentioned steps are for the assembly of the system in the unloaded condition.

10) To assemble in the loaded condition, fit Tygon tubing or some semi-stiff tubing to the output protrusion and attach the pump. See Figure 15 for additional details.

APPENDIX E

EQUIPMENT SPECIFICATIONS

A. CONTROLLER

Input: Thermocouple (Type J)

Accuracy: ± 0.5%

Proportioning Band: 2% of full scale

On/Off Differential: Less than 0.1% of range

Indicator Accuracy: ± 1%

Supply Voltage: 115 volts a.c.

B. OSCILLOGRAPH

Sensitivity: 10 mv per chart line (mm) full scale deflection from chart center, ± 200 mv.

Measurement Range: 0.010 Volts to 400 Volts

Amplifier Zero line Stability: Less than 1/10 chart line (mm) per hour when used with a pen oscillograph and chart paper. Total drift over an eight hour period is no more than 1/4 chart line (mm).

Sensitivity Steps: .01, .02, .05, .1, .2, .5, 1, 2, 5, and 10 volts per chart line (mm).

Frequency Response: The recorded peak-to-peak amplitude of a constant voltage sine wave will be within ± 1 chart line (mm) of a nominal 10 lines, from d.c. to 70 cps.

Calibration: Signal derived from an internal mercury cell.

Input Power required: 115 volts, 60 cps. (340 watts at 115 volts, 60 cps when all eight plug in amplifiers are in use.)

C. STRIP CHART RECORDER

Recording Mechanism: Servo-actuated ink pen drives; manually operated pen lift.

Response Time: One half second for full scale.

Chart Speeds: 1, 2 in/h; .1, .2, .5, 2 in/min; .1, .2, .5, 1, 2 in/sec.

Power: 115 volts, 60 Hz.

D. DIGITAL PYROMETER

Range: 0° to 750°F

Configuration: Potentometric with floating option.

Full Scale Voltage: 20 mv to 200 mv.

Reading Rate: Int. 3-6/sec, Ext. 0 to 3-6/sec.

Overall Error: 0.20%

Input Voltage: 115 volts $\pm$ 10%, 50/60 Hz.

E. PRESSURE TRANSDUCER

Linearity: $\pm$ ½% best straight line.

Overpressure: To 200% of range in either direction with less than ½% F.S. zero shift.

Output: 50 mv/v full scale nominal.

Temperature: Operating -65°F to 250°F
Compensated 0°F to 160°F

Pressure Cavity Volume: 0.004 in^3

Volumetric Displacement: 0.0003 in^3 for full scale.

F. DEMODULATOR

Power Requirements: 95 to 125 V ac, 50 to 400 Hz, 5 W

Output Signal: 0 to 10 V dc

Output Impedance: 2 K Ohms

Frequency Response: Flat from 0 to 1 K Hz, within $\pm$ 5%.

Temperature Range: +40% to + 120°F

LIST OF REFERENCES

1. United Kingdom Atomic Energy Authority Research
    Establishment, Harwell, Oxfordshire, England, The
    Fluidyne Heat Engine, by C. West, May 1971.

2. Office of Naval Research, London, England, Report No.
    AD - A006367, The Fluidyne Heat Engine: How to Build
    One, How it Works, by H. Elrod, December 1974.

3. United Kingdom Atomic Energy Authority Research
    Establishment, Harwell, Electronics and Applied
    Physics Division, Report No. AERE-M2840, The Onset
    of Oscillations in a Lossless Fluidyne, by A.D. Geisow,
    October 1976.

4. Drzewiecki, T.M., An Initial Model for the Finite
    Displacement Response Characteristics of a Fluidyne
    Pump, Project Leader, Fluid Control Branch, Harry
    Diamond Laboratories, January 1978.

INITIAL DISTRIBUTION LIST

No. Copies

1. Defense Documentation Center   2
    Cameron Station
    Alexandria, Virginia   22314

2. Library, Code 0142   2
    Naval Postgraduate School
    Monterey, California   93940

3. Department Chairman, Code 69   1
    Department of Mechanical Engineering
    Naval Postgraduate School
    Monterey, California   93940

4. Professor R. H. Nunn, Code 69Nn   5
    Department of Mechanical Engineering
    Naval Postgraduate School
    Monterey, California   93940

5. Professor D. Salinas, Code 69Zc   1
    Department of Mechanical Engineering
    Naval Postgraduate School
    Monterey, California   93940

6. LT David C. Mosby, USN   1
    5940 Tooley Street
    San Diego, California   92114